



**HAL**  
open science

## Early expansion of circulating granulocytic myeloid-derived suppressor cells predicts development of nosocomial infections in septic patients

Fabrice Uhel, Imane Azzaoui, Murielle Grégoire, Céline Pangault, Joelle Dulong, Jean-Marc Tadié, Arnaud Gacouin, Christophe Camus, Luc Cynober, Thierry Fest, et al.

### ► To cite this version:

Fabrice Uhel, Imane Azzaoui, Murielle Grégoire, Céline Pangault, Joelle Dulong, et al.. Early expansion of circulating granulocytic myeloid-derived suppressor cells predicts development of nosocomial infections in septic patients. *American Journal of Respiratory and Critical Care Medicine*, 2017, 196 (3), pp.315-327. 10.1164/rccm.201606-1143OC . hal-01480854

**HAL Id: hal-01480854**

**<https://univ-rennes.hal.science/hal-01480854>**

Submitted on 1 Mar 2017

**HAL** is a multi-disciplinary open access archive for the deposit and dissemination of scientific research documents, whether they are published or not. The documents may come from teaching and research institutions in France or abroad, or from public or private research centers.

L'archive ouverte pluridisciplinaire **HAL**, est destinée au dépôt et à la diffusion de documents scientifiques de niveau recherche, publiés ou non, émanant des établissements d'enseignement et de recherche français ou étrangers, des laboratoires publics ou privés.

# Early expansion of circulating granulocytic myeloid-derived suppressor cells predicts development of nosocomial infections in septic patients.

Fabrice Uhel, MD, PhD<sup>1,2,3</sup>, Imane Azzaoui, PhD<sup>3,4,5,6</sup>, Murielle Grégoire, PhD<sup>3,4,5,6</sup>, Céline Pangault, PharmD, PhD<sup>3,4,5,6</sup>, Joelle Dulong, MBiol<sup>3,4,5,6</sup>, Jean-Marc Tadié, MD, PhD<sup>1,2,3,5</sup>, Arnaud Gacouin, MD<sup>1,2</sup>, Christophe Camus, MD, PhD<sup>1,2</sup>, Luc Cynober, PharmD, PhD<sup>7</sup>, Thierry Fest, MD, PhD<sup>3,4,5,6</sup>, Yves Le Tulzo, MD, PhD<sup>1,2,3,5</sup>, Mikael Roussel, MD, PhD<sup>3,4,5,6</sup> and Karin Tarte, PharmD, PhD<sup>3,4,5,6</sup>

<sup>1</sup> CHU Rennes, Maladies Infectieuses et Réanimation Médicale, F-35033 Rennes, France

<sup>2</sup> Inserm, CIC-1414, Faculté de Médecine, Université Rennes 1, F-35043 Rennes, France.

<sup>3</sup> Inserm, U917, Faculté de Médecine, Université Rennes 1, F-35043 Rennes, France

<sup>4</sup> CHU Rennes, Pôle Biologie, F-35033 Rennes, France

<sup>5</sup> Université Rennes 1, UMR917, F-35043 Rennes, France

<sup>6</sup> EFS Bretagne, F-35016 Rennes, France

<sup>7</sup> AP-HP Hôpital Cochin, Service de Biochimie, and Dept Nutrition EA 4466, Faculté de Pharmacie Paris Descartes F-75014 Paris, France

## Corresponding author

Fabrice Uhel, Service des Maladies Infectieuses et Réanimation Médicale, CHU Pontchaillou, 2 rue Henri Le Guilloux, F-35033 Rennes Cedex 9, France; e-mail: [fabrice.uhel@chu-rennes.fr](mailto:fabrice.uhel@chu-rennes.fr); Phone: +33(0) 299 284 248; Fax: +33(0) 299 284 164.

Karin Tarte, INSERM U917, Faculté de Médecine, 2 Avenue du Pr Léon Bernard, F-35043 Rennes France, E-mail: [karin.tarte@univ-rennes1.fr](mailto:karin.tarte@univ-rennes1.fr), Phone: +33 (0) 223 234 512, fax: +33 (0) 223 234 958.

## Authors' contribution

Raised funds: FU, KT, TF. Designed and supervised research: KT, MR, TF, YLT. Designed experiments: FU, IA, JD, CP. Performed experiments: FU, IA, MG, LC. Provided samples: FU, JD, JMT, AG, CC, YLT. Analyzed data: FU, IA, JD, CP, JMT, AG, CC, MR, KT. Wrote the paper: FU, KT. Critically revised the manuscript: all authors.

## Grant support

This work was supported by research grants from the French Intensive Care Society (SRLF) and the National Institute of Cancer (INCa Recherche Translationnelle 2010).

## Descriptor numbers

4.12 – 7.08 – 7.19 – 10.07

## Running title

MDSC and nosocomial infections in septic patients

**Article word count:** 3966

**At a Glance Commentary**

*Scientific Knowledge on the Subject:* Sepsis is characterized by a persistent immune dysfunction responsible for nosocomial infections and poor outcome. The role of myeloid-derived suppressor cells (MDSCs), described as potent inhibitors of immune responses in cancer and inflammatory conditions, still needs to be clarified in septic patients.

*What This Study Adds to the Field:* We demonstrate that monocytic (M)-MDSCs are expanded in ICU septic and non-septic patients and that granulocytic (G)-MDSCs are more specifically expanded in septic patients. Both subsets independently inhibit T-cell proliferation. G-MDSCs are made of immature and mature granulocytes expressing high levels of degranulation markers and produce arginase 1. Importantly, early expansion of G-MDSCs, unlike M-MDSCs, is associated with subsequent occurrence of nosocomial infections, suggesting a major role for those cells in sepsis-induced immune suppression. MDSCs may thus become interesting therapeutic targets to restore immune capacities of septic patients.

(130 words)

This article has an online data supplement, which is accessible from this issue's table of content online at [www.atsjournals.org](http://www.atsjournals.org)

## ABSTRACT

**Rationale:** Sepsis induces a sustained immune dysfunction responsible for poor outcome and nosocomial infections. Myeloid-derived suppressor cells (MDSCs) described in cancer and inflammatory processes may be involved in sepsis-induced immune suppression but their clinical impact remains poorly defined.

**Objectives:** To clarify phenotype, suppressive activity, origin, and clinical impact of MDSCs in septic patients.

**Methods:** Peripheral blood transcriptomic analysis was performed on 29 septic patients and 15 healthy donors. A second cohort of 94 consecutive septic patients, 11 severity-matched intensive care patients and 67 healthy donors was prospectively enrolled for flow cytometry and functional experiments.

**Measurements and Main Results:** Genes involved in MDSC suppressive functions, including *S100A12*, *S100A9*, *MMP8* and *ARG1*, were upregulated in the peripheral blood of septic patients. CD14<sup>pos</sup>HLA-DR<sup>low/neg</sup> monocytic (M)-MDSCs were expanded in intensive care septic and non-septic patients and CD14<sup>neg</sup>CD15<sup>pos</sup> low-density granulocytes/ granulocytic (G)-MDSCs were more specifically expanded in septic patients ( $p < .001$ ). Plasma levels of MDSC mediators S100A8/A9, S100A12, and Arginase 1 were significantly increased. *In vitro*, CD14<sup>pos</sup>- and CD15<sup>pos</sup>-cell depletion increased T-cell proliferation in septic patients. G-MDSCs, made of immature and mature granulocytes expressing high levels of degranulation markers, were specifically responsible for arginase 1 activity. High initial levels of G-MDSCs, arginase 1, and S100A12 but not M-MDSCs were associated with subsequent occurrence of nosocomial infections.

**Conclusions:** M-MDSCs and G-MDSCs strongly contribute to T-cell dysfunction in septic patients. More specifically, G-MDSCs producing arginase 1 are associated with a higher incidence of nosocomial infections and appear to be major actors of sepsis-induced immune suppression.

**Abstract word count:** 247

**Keywords:** Sepsis, granulocytes, monocytes, cross infection, immune tolerance.

## INTRODUCTION

Sepsis is one of the leading causes of admission in intensive care units (ICUs). Despite a decreased overall mortality rate during the past three decades, the prognosis remains hampered by a high long term mortality secondary to nosocomial infections with opportunistic pathogens or viral reactivations, an increased risk of cardiovascular events and cancers, and frequent hospital readmissions causing increased healthcare costs (1-4). This unfavorable outcome has been largely attributed to a persistent immunological impairment affecting both innate and adaptive immunity (5). To date, the most described features are *i*) monocyte dysfunction illustrated by reduced expression of HLA-DR and impaired production of inflammatory cytokines after bacterial challenge *in vitro* (6, 7), *ii*) granulocyte functional impairment (8), *iii*) lymphopenia and lymphocyte dysfunction associated with an increased proportion of regulatory T-cells (Tregs) (9, 10) and *iv*) enhanced systemic indoleamine 2,3-dioxygenase (IDO) activity (11).

During the past decade, much attention has focused on a heterogeneous population of cells from the myeloid lineage called myeloid-derived suppressor cells (MDSCs) which have been demonstrated to play potent immunosuppressive functions in cancers and inflammatory diseases (12, 13). In cancer, they are induced by many soluble factors (such as S100A8/A9, GM-CSF, G-CSF, IL-6, IL-10, VEGF or TGF- $\beta$ ) as a consequence of a maturational block and/or dysregulated myelopoiesis. Various mechanisms have been proposed to explain their suppressive activity, including depletion of arginine and tryptophan by arginase 1 and IDO, respectively; production of reactive oxygen species (ROS) by NADPH oxidase; release of IL-10 or

TGF- $\beta$ ; and induction of Tregs (14-17). Two main subsets, monocytic (M)-MDSCs and granulocytic (G)-MDSCs, have been identified, but their definition and role in humans remain elusive due to the lack of specific phenotypic markers (18).

CD14<sup>pos</sup>HLA-DR<sup>low/neg</sup> cells described more than 15 years ago as TLR-unresponsive cells in septic patients were recently reconsidered as M-MDSCs (19) but were not evaluated for their suppressive functions. Conversely, G-MDSCs with various phenotypes, including CD15<sup>pos</sup> cells with decreased CD10 and CD16 expression, Lin<sup>neg</sup>CD33<sup>pos</sup>CD15<sup>pos</sup>HLA-DR<sup>neg</sup> cells, or CD15<sup>pos</sup> low-density granulocytes (LDGs) that co-purify with peripheral blood mononuclear cells (PBMCs) after density gradient centrifugation, were shown to be expanded in septic and in ICU non-septic patients, and to display T-cell inhibitory activity (20-22). Especially, CD15<sup>pos</sup> LDGs were recently proposed to variably display either arginase or ROS-dependent inhibitory effects with a potential impact of causative pathogens (19, 20). However, the low number of patients studied and the controversial phenotype and origin of putative suppressor cells preclude any definitive conclusion on the clinical impact, mechanisms of action, and role of MDSCs in septic patients.

Consequently, our objectives were *i*) to highlight the various putative MDSC subsets within the circulating myeloid compartment, *ii*) to characterize their suppressive activity, *iii*) to clarify their origins, and *iv*) to study their clinical impact in septic patients.

## **MATERIALS AND METHODS**

### *Patients and healthy donor participants*

This study was performed in the ICU at Rennes University Hospital. 94 consecutive adult septic patients and 11 severity-matched ICU non-septic patients were prospectively enrolled, and compared with 67 healthy donors. The study design was approved by the local institutional review board and written informed consents were obtained. Pregnant women, patients younger than 18 years old, patients with malignancy, HIV infection, or receiving immunosuppressive agents were excluded. The standard criteria were used for diagnosis of severe sepsis and septic shock (23). The Simplified Acute Physiology Score (SAPS II), the Sepsis-related Organ Failure Assessment (SOFA) score and the Logistic Organ Dysfunction (LOD) system at admission in ICU were used to assess sepsis severity (24-26). Patients received standard enteral or parenteral nutrition. The occurrence of nosocomial infections during hospitalization was recorded prospectively and defined as previously described (27).

### *Samples*

Blood heparinized samples were collected within 3 days following sepsis diagnosis. The delay between sampling and beginning of laboratory procedures was <1h. PBMCs were isolated by Ficoll density gradient, and plasma samples were stored at -80°C until use. Whole blood RNA samples collected on PAXGene Blood RNA tubes (PreAnalytiX) at the same time-point came from a previously published cohort of septic patients with similar inclusion/exclusion criteria (11) and were stored at -80°C before RNA extraction.

### *Flow cytometry*

White blood cell differentials were obtained using the Cytodiff™ panel (Beckman Coulter) (28). Myeloid subpopulations including MDSCs were then quantified on whole blood or PBMCs using multicolor antibody panels and Flow-count fluorospheres (Beckman Coulter) (*Table E1*). Samples were run on a Navios flow cytometer and data were analyzed using Kaluza software (Beckman Coulter). Gating strategy was defined as previously described (*Figure E1*) (29).

### *Quantitative real-time PCR*

Quantitative RT-PCR were performed on whole blood RNA using Taqman array custom microfluidic cards (Applied Biosystems) and on purified granulocyte subsets using Fluidigm system. Methods are detailed in the online data supplement.

### *Cytokines and enzymes activity assessment*

Plasma levels of Myeloperoxidase (MPO), neutrophil gelatinase-associated lipocalin (NGAL) (R&D Systems), S100A8/9, S100A12, and Arginase I (Hycult Biotech) were determined by ELISA. Plasma levels of G-CSF, IL-10, and IL-12 were measured using a Milliplex map magnetic bead kit (EMD Millipore). IDO and arginase activities were respectively evaluated by measuring kynurenine and tryptophan levels by high-performance liquid chromatography, and ornithine and arginine concentrations by ion-exchange chromatography (11, 30).

### *Cell isolation and culture*

Proliferation of T cells from whole or CD14/CD15-depleted PBMCs was assessed by CFSE dilution. Details are provided in the online data supplement. For cytological analyses, cytospin slides were stained with May-Grünwald-Giemsa.

### *Statistical analysis*

Statistical analyses were performed with GraphPad Prism 6.0 software. Comparisons between groups were performed using Mann-Whitney *U* test, Wilcoxon matched-pairs signed test for matched samples. Kruskal-Wallis or Friedman (matched samples) with Dunn's correction tests were performed if multiple comparisons were requested. Correlations between continuous variables were investigated using nonparametric Spearman rank correlation test. Unsupervised hierarchical clustering with Spearman's rank distance and average linkage was performed using Cluster 3.0 (31). Results were displayed using Treeview (<http://jtreeview.sourceforge.net>). A receiver operating characteristic (ROC) plot was performed to determine the best G-MDSC threshold to discriminate between patients with high *versus* low risk of nosocomial infections. Kaplan-Meier curves were compared with the Mantel-Cox log-rank test. Gene set enrichment analysis (GSEA) was performed using the BROAD Institute GSEA software (<http://www.broad.mit.edu/gsea/>) on a previously published dataset of septic patients (GSE65682) using the panel of genes defined for the TLDA analyses.

## RESULTS

*Peripheral blood transcriptomic analysis reveals a myeloid suppressive signature in septic patients.*

A transcriptomic analysis targeting 44 immune-related genes, including cell subset specific markers and functional pathways, was conducted on a previously published cohort of 29 septic patients and 15 healthy donors. Unsupervised hierarchical clustering analysis discriminated septic patients from healthy donors (*Figure 1A*). More importantly, genes associated with MDSC recruitment, phenotype, and suppressive functions, including *MMP8*, *MMP9*, *ARG1*, *S100A8*, *S100A9*, *S100A12*, *CD274* (PD-L1), *IL4R*, and *IL10* were upregulated whereas genes associated with adaptive immunity and inflammation, including *CD4*, *MS4A1* (CD20), *CD8B*, *CD3G*, *IL8*, and *IL6* were downregulated in septic patients (*Table 1*). A gene set enrichment analysis (GSEA) confirmed that upregulated genes were enriched in a large external cohort of septic patients (32) (*Figure 1B*). Of note, a hierarchical clustering analysis performed among septic patients could not find any segregation according to the severity of illness, *i.e.* septic shock *versus* severe sepsis (*Figure E2*). *ARG1* and *S100A9* expression correlated with granulocyte count and inversely correlated with lymphocyte count (*Figure 1C*). Noteworthy, even if both *CD247* (CD3 $\zeta$ ) and *CD3G* (CD3 $\gamma$ ) were downregulated, the *CD247/CD3G* ratio was further decreased in septic patients and inversely correlated with granulocyte count (*Figure 1D*). Those data raise the hypothesis that a suppressive activity burden by myeloid cells may impair T-cell count and functions in septic patients.

*Peripheral blood myeloid cells display a suppressive phenotype in septic patients.*

To further study the potential role of myeloid cells in sepsis-induced immune dysfunction, we set up an independent prospective cohort of 94 septic patients and 67 healthy donors. The population characteristics are summarized in *Table 2* and sepsis etiology is detailed in *Table 3*. As human MDSCs are heterogeneous and poorly defined, we started by performing an extensive description of the circulating myeloid compartment in a cohort of 36 septic patients and 26 healthy donors (*Figure 2A*). As previously described (11), the CD14<sup>pos</sup> monocyte count was increased in septic patients compared to healthy donors. Interestingly, this difference was essentially related to the CD14<sup>pos</sup>CD16<sup>pos</sup> subtype ( $p < .001$ ). Moreover, consistently with previous reports, the inflammatory CD14<sup>dim</sup>CD16<sup>pos</sup> subset was strongly decreased ( $p < .001$ ) (33). As expected, HLA-DR expression in septic patients was decreased on all monocyte subtypes ( $p < .001$ ) (*Figures E3A & E3B*). In agreement, the number of CD14<sup>pos</sup>HLA-DR<sup>low/neg</sup> monocytes, previously described as M-MDSCs, was markedly increased in septic patients ( $143.2 \times 10^6/L$  [Interquartile range (IQR),  $35.7-340.9 \times 10^6/L$ ]) compared to healthy donors ( $4.0 \times 10^6/L$  [IQR,  $2.0-17.5 \times 10^6/L$ ],  $p < .001$ ). Besides an increase in circulating mature and immature granulocytes ( $p < .001$ ), we observed in septic patients a high proportion of CD14<sup>neg</sup>CD15<sup>pos</sup> LDGs (28.7% of PBMCs [IQR, 18.2-52.9%] in septic patients, vs. .8% [IQR, .31-2.1%] in healthy donors,  $p < .001$ ), previously described as G-MDSCs (34). The absolute LDG count was also increased in septic patients. Interestingly, both proportion ( $\rho = .35$ ,  $p = .005$ ) and absolute count ( $\rho = .44$ ,  $p < .001$ ) of LDGs correlated with immature unlike mature granulocyte counts. The CD14<sup>pos</sup>HLA-DR<sup>low/neg</sup> count and the proportion of LDGs did not correlate. These subsets were not statistically different

between severe sepsis and septic shock patients (data not shown). Importantly, whereas M-MDSC were significantly increased in ICU non-septic patients ( $p < .001$ ), raising a similar level than in septic patients, G-MDSCs increase was more specific to septic patients (*Figure 2B*) and persisted for at least 14 days (*Figure E3C*). Of note, whereas the proportion of LDGs did not differ according to the Gram staining of the causative microorganism, the number of circulating  $CD14^{pos}HLA-DR^{low/neg}$  monocytes was higher in patients with Gram-negative sepsis (*Figure E3D*). Lastly, the three dendritic cell (DC) subtype counts (plasmacytoid DC, and both subsets of myeloid DC expressing CD1c or CD141) were dramatically decreased in septic patients (*Figure E4A*).

To confirm and extend this work, we studied the characteristic features of MDSC activity at the protein level (*Figure 2C*). In agreement with their increased RNA levels in peripheral blood, concentrations of calcium-binding proteins S100A8/A9 and S100A12 involved in MDSC recruitment (35) were increased in the peripheral blood of septic patients ( $p < .001$ ). Plasma level of G-CSF, which has been reported to take part in the recruitment of G-MDSCs (36), was also increased in septic patients ( $p = .001$ ). The plasma kynurenine/tryptophan ratio reflecting IDO activity was markedly increased in patients with sepsis (.213 [IQR, .092-.658], +719%,  $p < .001$ ) compared with healthy donors (.026 [IQR, .023-.035]). As previously described, this increase was not associated with an upregulation of *IDO1* expression (data not shown)(11). Conversely, plasma levels of arginase 1 were increased in septic patients (119.3 ng/mL [IQR, 68.2-242.5 ng/mL], vs. 18.3 ng/mL [IQR, 9.6-23.4 ng/mL],  $p < .001$ ), correlated with immature granulocyte count ( $\rho = .28$ ,  $p = .03$ ) and

were associated with a decreased arginine concentration (35.3  $\mu\text{mol/L}$  [IQR, 23.9-59.7  $\mu\text{mol/L}$ ] vs. 66.5  $\mu\text{mol/L}$  [IQR, 52.1-95.1  $\mu\text{mol/L}$ ],  $p < .001$ ). Finally, the increased IL10/IL12 ratio at protein and transcriptomic levels was consistent with an overall suppressive environment (*Figure E4B*), as highlighted by the significant decrease in the various lymphocyte subsets (*Figure E4C*).

Altogether, these data indicate a similar expansion of  $\text{CD14}^{\text{pos}}\text{HLA-DR}^{\text{low/neg}}$  monocytes in ICU septic and non-septic patients, and a more intense and specific increase of  $\text{CD15}^{\text{pos}}\text{CD14}^{\text{neg}}$  LDGs in septic patients. Those subsets are consistent with M-MDSC and G-MDSC phenotypes respectively, and occur in a systemic suppressive environment.

*CD14<sup>pos</sup> monocytes and CD15<sup>pos</sup> LDGs from septic patients display a MDSC activity in vitro.*

As MDSC definition in humans lacks phenotypic specificity and relies on their suppressive properties, we next assessed the influence of  $\text{CD14}^{\text{pos}}$  and  $\text{CD15}^{\text{pos}}$  cells on T-cell proliferation. The proliferation of both  $\text{CD4}^{\text{pos}}$  and  $\text{CD8}^{\text{pos}}$  T-cells was strongly reduced in septic patients (*Figure 3A*). Depletion of  $\text{CD14}^{\text{pos}}$  cells resulted in a significant increase in the proportion of proliferating  $\text{CD4}^{\text{pos}}$  (+144%,  $p = .002$ ) and  $\text{CD8}^{\text{pos}}$  (+124%,  $p = .004$ ) T-cells in septic patients, whereas it was associated with a decreased  $\text{CD4}^{\text{pos}}$  and  $\text{CD8}^{\text{pos}}$  T-cell proliferation in healthy donors (-15%,  $p = .02$  and -17%,  $p = .008$ ; respectively) (*Figures 3B & E5*). Similarly, depletion of  $\text{CD15}^{\text{pos}}$  cells in septic patients increased  $\text{CD4}^{\text{pos}}$  and  $\text{CD8}^{\text{pos}}$  T-cell proliferation by +60% ( $p = .014$ ) and +65% ( $p = .037$ ) respectively, whereas it had no effect on healthy donor T-cell proliferation, in agreement with the lack of LDGs in normal context. These results

indicate that both CD14<sup>pos</sup> monocytes, essentially made up of HLA-DR<sup>low/neg</sup> cells, and CD15<sup>pos</sup> LDGs should be considered as MDSCs in sepsis. We then assessed if sepsis-related MDSCs displayed Arginase 1 activity by measuring arginine and ornithine concentrations in culture supernatants. PBMCs from septic patients but not those from healthy donors exerted an Arginase 1 activity *in vitro*, as demonstrated by an increased ornithine/arginine ratio ( $p=.009$ ). This activity was completely abrogated after CD15<sup>pos</sup> LDG depletion but was not affected by CD14<sup>pos</sup> monocyte depletion ( $p<.001$ ) (*Figure 3C*). In addition, arginase activity strongly correlated with the number of LDGs in culture ( $\rho=.90$ ,  $p<.001$ ) further reinforcing the demonstration that LDGs, unlike monocytes, are key arginase 1 producers in septic patients.

#### *High initial levels of G-MDSC are associated with a higher risk of secondary nosocomial infections*

Among septic patients, 21 (22%) developed one or more nosocomial infection during hospital stay (*Table E2*). The first episode occurred 6 days after ICU admission (median 20 days [IQR, 12-28 days]). The initial proportion of LDGs correlated with SOFA score ( $\rho=.28$ ,  $p=.019$ ) and was significantly higher in patients who further developed nosocomial infections (45.5% of PBMCs [IQR, 24.5-69.4%] compared to patients who did not (26.5% [IQR, 16.3-45.7%,  $p=.008$ ) (*Figure 4A*). Similarly, the initial peripheral immature granulocyte count was 2.5 fold higher ( $2.1 \times 10^6/L$  [IQR,  $.6-4.3 \times 10^6/L$ ] in patients with nosocomial infections vs.  $.9 \times 10^6/L$  [IQR,  $.3-2.3 \times 10^6/L$ ] in patients without nosocomial infections,  $p=.046$ ) whereas the mature granulocyte count was not significantly different. A ROC plot determined that LDGs>36% was the best threshold to identify patients with the highest risk of

developing nosocomial infections (area under the curve (AUC) .70 (95% confidence interval [CI] .57-.83). The cumulative incidence of nosocomial infections was thus significantly higher in patients with LDGs>36% (Hazard ratio 2.83; 95%CI 1.18–8.11; Log rank  $p=.023$ ). Conversely, the peripheral CD14<sup>pos</sup>HLA-DR<sup>low/neg</sup> monocyte count was not associated with nosocomial infection occurrence (*Figure 4B*).

In line with those results, development of nosocomial infections was also associated with higher initial plasma concentrations of S100A12 ( $p=.027$ ) and G-CSF ( $p=.013$ ) (*Figure 4C*). More importantly, early levels of arginase 1, specifically produced by G-MDSCs, correlated with initial SOFA ( $\rho=.49$ ,  $p=.011$ , Spearman) and SAPS II ( $\rho=.41$ ,  $p=.035$ , Spearman) scores, and were significantly higher in patients who developed nosocomial infections ( $p=.043$ ).

*Low-density granulocytes in septic patients are composed of immature and mature granulocytes expressing high levels of degranulation markers.*

Given the importance of LDGs in the outcome of septic patients, we finally sought to better characterize them. Detailed phenotypic phenotyping of LDGs revealed high expression of CD11b ( $\alpha$ M-integrin, expressed by mice MDSCs) and CD64 (Fc $\gamma$ RI, upregulated on myeloid cells from septic patients (41)), and intermediate levels of CD33 and CD115 (colony-stimulating factor 1 receptor). We also observed two levels of CD16 expression, consistent with mature and immature stages (*Figure E6A*).

As granulocytes that co-purify in the PBMC-fraction were called LDGs, we referred to granulocytes which sediment with erythrocytes as high-density granulocytes (HDGs). To determine if LDGs and HDGs could be morphologically and

phenotypically distinguished, we compared CD15<sup>pos</sup> cells from density gradient interface (LDGs) and pellet (HDGs). Based on their expression of CD16 and CD11b maturation markers, we noticed that LDGs were significantly enriched for immature granulocytes (*Figure 5A*). Indeed, LDGs contained a higher proportion of CD15<sup>pos</sup>CD16<sup>neg</sup>CD11b<sup>pos/low</sup> promyelocytes and myelocytes (4.4±2.3% vs. .4±.2%, p=.004), a higher proportion of CD15<sup>pos</sup>CD16<sup>low</sup> metamyelocytes (51.5±12.3% vs. 38.9±12.1%, p=.008) and a lower proportion of mature neutrophils (44.0±13.5% vs. 60.7±12.2%, p=.004) compared to HDGs. Morphological analysis confirmed that HDGs could be considered as a homogeneous population of mature neutrophils, whereas LDGs were composed of neutrophils at different stages of maturation, including mature segmented neutrophils as well as more immature banded neutrophils and myelocytes (*Figure 5B*). Consistently, qPCR performed on paired HDGs/LDGs from 5 septic patients showed a higher expression of genes involved in early granulocytic maturation in LDGs (*CEBPE*, *CEBPA*, and *RUNX1*) (*Figure 5C*).

Since arginase 1 has been previously shown to be stocked inside azurophilic granules of human granulocytes (37), we hypothesized that LDGs might result from neutrophil activation and degranulation. As compared to HDGs, LDGs expressed higher surface levels of CD35 (p<.05), CD63 (p<.01) and CD66b (p<.01) on both mature and immature subsets, indicating degranulation of secretory vesicles, azurophilic, and specific granules; respectively (38) (*Figure 5D*). Furthermore, LDGs had lower side and forward scatter (SSC and FSC) than HDGs, suggesting that they were smaller and had lower granularity (*Figures 5E, E6B*). Consistently, plasma levels of neutrophil granule proteins MPO and NGAL were significantly increased in septic patients compared to healthy donors (p<.001) (*Figure 5F*).

## DISCUSSION

A vast majority of patients surviving the initial phase of sepsis display signs of immune suppression directly related to persistent lymphopenia and T-cell exhaustion (39, 40). In this study, we demonstrated that CD14<sup>pos</sup>HLA-DR<sup>low/neg</sup> M-MDSCs were expanded in ICU septic and non-septic patients and that CD14<sup>neg</sup>CD15<sup>pos</sup> LDGs/G-MDSCs were more specifically expanded in septic patients. Both subsets independently inhibited T-cell proliferation *in vitro*. Especially, G-MDSCs responsible for an arginase activity were composed of immature and mature granulocytes displaying high levels of degranulation markers. More importantly, we demonstrated that the early expansion of G-MDSC predicted the development of nosocomial infections in septic patients.

Of note, our conclusions were based on a single center exploratory study. Despite the relatively large number of patients included, the design and the number of events did not allow to perform a reliable multivariate analysis of risk factors associated with ICU-acquired infections. A multicentric study will allow confirming the specific role of G-MDSCs in the promotion of nosocomial infections in septic patients.

The decreased expression of HLA-DR on monocytes has been associated with poor prognosis and increased risk of nosocomial infections, and is currently considered an essential surrogate marker of monocyte unresponsiveness (41). "Endotoxin tolerance", defined by the reduced capacity of monocytes to release pro-inflammatory cytokines associated with a preserved or enhanced ability to release

anti-inflammatory mediators in response to bacterial compounds, has thus been one of the most described features of sepsis-induced immunosuppression (42). For the first time, we described CD14<sup>pos</sup>HLA-DR<sup>low/neg</sup> monocytes not only as hypo-responsive cells, but also as actively suppressive M-MDSCs. Indeed, as previously described in cancer patients, we demonstrated that CD14<sup>pos</sup>HLA-DR<sup>low/neg</sup> monocytes were responsible for a strong inhibition of T-cell proliferation *in vitro*. However, we only found a trend toward higher initial number of peripheral M-MDSCs in patients who further developed nosocomial infections. This result could be explained by the fact that only persisting but not initial low monocyte HLA-DR expression predicts mortality in septic shock (7, 43). Moreover, we demonstrated that expansion of M-MDSC was not specific to septic patients and could reflect a more global response to injury in ICU patients. As described in mice, stress-induced endogenous production of cortisol, as well as corticosteroid medications, could be involved in this process (44). Consequently, the precise role of those cells during immune response as well as their mechanisms of action deserves to be further described.

Besides M-MDSCs, granulocyte subsets also appear to display potent suppressive functions during sepsis. To date, neutrophils had been mainly shown to be affected by a severe dysfunction, including impaired capacities of bacterial clearance, reduced production of ROS and decreased recruitment to infected tissues (45). Patients with the most severe dysfunction were more vulnerable to nosocomial infections (8). As recently reported, we found a high proportion of LDGs/G-MDSCs in septic patients compared to healthy donors (19, 20, 46). Moreover, we revealed for the first time that this increased in G-MDSC was much stronger in septic patients

than in severity-matched non-septic ICU patients and should thus be considered as a more specific feature of the septic immune microenvironment. G-MDSCs were specifically responsible for an arginase activity. They were associated with a decreased CD3 $\zeta$  chain expression, and were directly able to inhibit T-cell proliferation. Unlike previously described, we didn't find any association with the Gram staining of the causative organism (19). This discrepancy may be explained by the larger size of our cohort, reflecting a higher diversity of infections. Arginase is one of the most described mechanisms of MDSC-mediated suppression (16). However, we cannot exclude that other mechanisms such as ROS production or PD-L1 expression could also be involved in septic patients. In agreement, arginase 1 inhibition failed to restore T-cell proliferation *in vitro* (data not shown) and CD274/PD-L1 expression was increased in the peripheral blood of septic patients.

Although LDGs have been described as a unique population of granulocytes that co-purify with PBMCs after density centrifugation, their origins in septic patients remained unclear. We demonstrated that G-MDSC consisted of both immature and mature cells displaying high levels of degranulation markers. As previously described, the immature subset may originate from the bone marrow as a result of emergency myelopoiesis (47). Consistently, we found high levels of G-CSF in the plasma from septic patients. Thus, simultaneously to the reconstitution and expansion of the primary granulocytic compartment, development of G-MDSCs may represent an important mechanism of regulation of the immune response. Accordingly, a recent prospective immunomonitoring study revealed that circulating immature granulocytes predicted early sepsis deterioration and could be responsible

for immunosuppression through the induction of T-cell lymphopenia (21). Besides this process of increased myelopoiesis, animal studies strongly suggest the existence of an early disruption of myeloid maturation and differentiation (47, 48). Especially, persistent inflammatory environment like cancer or sepsis may prevent MDSC from further differentiating into mature myeloid cells. Contrary to the initial statement that defined MDSCs as immature cells, we demonstrated that G-MDSCs were also composed of mature cells, expressing high levels of degranulation markers and displaying lower size and granularity than HDGs. This phenotype may reflect an alternate activation state resulting in the release of suppressive molecules such as arginase 1 from intracellular granules to the circulation. Those results are consistent with previous description of LDGs in patients with HIV infection or renal cell carcinomas (49, 50). Conversely, in a mouse tumor model, *Sagiv et al.* demonstrated that mature LDGs may also derive from HDGs upon TGF- $\beta$  stimulation but not by a degranulation process (51), suggesting a high diversity and plasticity of granulocytes, depending on various pathological processes.

Importantly, we demonstrated that a high level of G-MDSCs at the initial phase of sepsis predicted the development of subsequent nosocomial infections in medical-ICU septic patients. Arginase 1 produced by G-MDSCs plays a major role in the plasma arginine depletion (the so-called arginine-deficiency syndrome (52)) and the subsequent poor prognosis, as previously described in ICU non-septic patients (22). Granulocytes that have been considered for a long while as primary short-lived effectors of the host defense appear to display an important plasticity during sepsis. The massive recruitment of neutrophils from the bone marrow combined with a

delayed apoptosis results in a markedly increased number of circulating neutrophils of various degrees of maturation (53, 54). Pathogen-derived factors as well as endogenous alarmins such as S100 proteins may subsequently promote polarization of specific subpopulations towards suppressive phenotypes. Of note, MDSC counts were not significantly different between survivors and non-survivors (data not shown). This result might be explained by the important decrease in sepsis mortality during the past decades (1). Moreover, a large prospective observational study recently demonstrated that ICU-acquired infections contributed only modestly to overall mortality (55). Consequently, occurrence of nosocomial infections might be a more relevant endpoint than overall mortality regarding consequences of sepsis-induced immunosuppression.

## **CONCLUSIONS**

Altogether, our results show that MDSCs are major actors of the sepsis-induced immune suppression. CD14<sup>pos</sup>HLA-DR<sup>low/neg</sup> M-MDSCs and CD15<sup>pos</sup> G-MDSCs strongly contribute to T-cell dysfunction in septic patients and the early expansion of arginase-1-producing G-MDSCs specifically promotes the development of nosocomial infections. Controlling the expansion of MDSCs or blocking their suppressive functions may represent promising novel therapeutic approaches in sepsis, as currently developed for cancer (56-58).

## **ACKNOWLEDGEMENTS**

We are thankful for the clinicians of the Polyvalent ICU of Saint Briec, of the Surgical and ICU of Rennes and for the French Blood Bank (EFS) of Rennes for providing samples. The authors acknowledge the Centre de Ressources Biologiques (CRB-santé) of Rennes (BB-0033-00056, <http://www.crbsante-rennes.com>) for managing samples, and all patients who participated in this study.

## **AUTHOR DISCLOSURES**

The authors declare no competing financial interest

## REFERENCES

1. Kaukonen K-M, Bailey M, Suzuki S, Pilcher D, Bellomo R. Mortality Related to Severe Sepsis and Septic Shock Among Critically Ill Patients in Australia and New Zealand, 2000-2012. *JAMA* 2014;311:1308.
2. Luyt C-E, Combes A, Deback C, Aubriot-Lorton M-H, Nieszkowska A, Trouillet J-L, Capron F, Agut H, Gibert C, Chastre J. Herpes Simplex Virus Lung Infection in Patients Undergoing Prolonged Mechanical Ventilation. *Am J Respir Crit Care Med* 2007;175:935–942.
3. Yende S, D'Angelo G, Kellum JA, Weissfeld L, Fine J, Welch RD, Kong L, Carter M, Angus DC. Inflammatory Markers at Hospital Discharge Predict Subsequent Mortality after Pneumonia and Sepsis. *Am J Respir Crit Care Med* 2008;177:1242–1247.
4. Ou S-M, Chu H, Chao P-W, Lee Y-J, Kuo S-C, Chen T-J, Tseng C-M, Shih C-J, Chen Y-T. Long-term Mortality and Major Adverse Cardiovascular Events in Sepsis Survivors: A Nationwide Population-based Study. *Am J Respir Crit Care Med* 2016;rccm.201510–2023OC–80.doi:10.1164/rccm.201510-2023OC.
5. Hotchkiss RS, Monneret G, Payen D. Sepsis-induced immunosuppression: from cellular dysfunctions to immunotherapy. *Nat Rev Immunol* 2013;13:862–874.
6. Rigato O, Salomao R. Impaired production of interferon-gamma and tumor necrosis factor-alpha but not of interleukin 10 in whole blood of patients with sepsis. *Shock* 2003;19:113–116.
7. Le Tulzo Y, Pangault C, Amiot L, Guilloux V, Tribut O, Arvieux C, Camus C, Fauchet R, Thomas R, Drénou B. Monocyte Human Leukocyte Antigen–DR Transcriptional Downregulation by Cortisol during Septic Shock. *Am J Respir Crit Care Med* 2004;169:1144–1151.
8. Stephan F, Yang K, Tankovic J, Soussy C-J, Dhonneur G, Duvaldestin P, Brochard L, Brun-Buisson C, Harf A, Delclaux C. Impairment of polymorphonuclear neutrophil functions precedes nosocomial infections in critically ill patients. *Crit Care Med* 2002;30:315–322.
9. Le Tulzo Y, Pangault C, Gacouin A, Guilloux V, Tribut O, Amiot L, Tattevin P, Thomas R, Fauchet R, Drénou B. Early circulating lymphocyte apoptosis in human septic shock is associated with poor outcome. *Shock* 2002;18:487–494.
10. Venet F, Chung C-S, Kherouf H, Geeraert A, Malcus C, Poitevin F, Bohé J, Lepape A, Ayala A, Monneret G. Increased circulating regulatory T cells (CD4(+)CD25 (+)CD127 (-)) contribute to lymphocyte anergy in septic shock patients. *Intensive Care Med* 2009;35:678–686.
11. Tattevin P, Monnier D, Tribut O, Dulong J, Bescher N, Mourcin F, Uhel F, Le Tulzo Y, Tarte K. Enhanced indoleamine 2,3-dioxygenase activity in patients with severe sepsis and septic shock. *J Infect Dis* 2010;201:956–966.
12. Gabrilovich DI, Nagaraj S. Myeloid-derived suppressor cells as regulators of the immune system. *Nat Rev Immunol* 2009;9:162–174.

13. Solito S, Marigo I, Pinton L, Damuzzo V, Mandruzzato S, Bronte V. Myeloid-derived suppressor cell heterogeneity in human cancers. In: Rose NR, editor. *Ann N Y Acad Sci* 2014;1319:47–65.
14. Huang B. Gr-1+CD115+ Immature Myeloid Suppressor Cells Mediate the Development of Tumor-Induced T Regulatory Cells and T-Cell Anergy in Tumor-Bearing Host. *Cancer Research* 2006;66:1123–1131.
15. Mougiakakos D, Jitschin R, Bahr von L, Poschke I, Gary R, Sundberg B, Gerbitz A, Ljungman P, Le Blanc K. Immunosuppressive CD14+HLA-DRlow/neg IDO+ myeloid cells in patients following allogeneic hematopoietic stem cell transplantation. *Leukemia* 2013;27:377–388.
16. Rodríguez PC, Quiceno DG, Zabaleta J, Ortiz B, Zea AH, Piazuelo MB, Delgado A, Correa P, Brayer J, Sotomayor EM, Antonia S, Ochoa JB, Ochoa AC. Arginase I production in the tumor microenvironment by mature myeloid cells inhibits T-cell receptor expression and antigen-specific T-cell responses. *Cancer Research* 2004;64:5839–5849.
17. Schmielau J, Finn OJ. Activated granulocytes and granulocyte-derived hydrogen peroxide are the underlying mechanism of suppression of t-cell function in advanced cancer patients. *Cancer Research* 2001;61:4756–4760.
18. Damuzzo V, Pinton L, Desantis G, Solito S, Marigo I, Bronte V, Mandruzzato S. Complexity and challenges in defining myeloid-derived suppressor cells. *Cytometry* 2014;88:77–91.
19. Janols H, Bergenfelz C, Allaoui R, Larsson A-M, Rydén L, Björnsson S, Janciauskiene S, Wullt M, Bredberg A, Leandersson K. A high frequency of MDSCs in sepsis patients, with the granulocytic subtype dominating in gram-positive cases. *J Leukoc Biol* 2014;96:685–693.
20. Darcy CJ, Minigo G, Piera KA, Davis JS, McNeil YR, Chen Y, Volkheimer AD, Weinberg JB, Anstey NM, Woodberry T. Neutrophils with myeloid derived suppressor function deplete arginine and constrain T cell function in septic shock patients. *Crit Care* 2014;18:R163.
21. Guérin E, Orabona M, Raquil M-A, Giraudeau B, Bellier R, Gibot S, Béné M-C, Lacombe F, Droin N, Solary E, Vignon P, Feuillard J, Francois B. Circulating Immature Granulocytes With T-Cell Killing Functions Predict Sepsis Deterioration\*. *Crit Care Med* 2014;42:2007–2018.
22. Gey A, Tadie J-M, Caumont-Prim A, Hauw-Berlemont C, Cynober L, Fagon J-Y, Terme M, Diehl J-L, Delclaux C, Tartour E. Granulocytic myeloid-derived suppressor cells inversely correlate with plasma arginine and overall survival in critically ill patients. *Clin Exp Immunol* 2015;180:280–288.
23. Levy MM, Fink MP, Marshall JC, Abraham E, Angus D, Cook D, Cohen J, Opal SM, Vincent J-L, Ramsay G. 2001 SCCM/ESICM/ACCP/ATS/SIS International Sepsis Definitions Conference. *Crit Care Med* 2003;31:1250–1256.
24. Le Gall JR, Lemeshow S, Saulnier F. A new Simplified Acute Physiology Score (SAPS II) based on a European/North American multicenter study. *JAMA* 1993;270:2957–2963.

25. Le Gall JR, Klar J, Lemeshow S, Saulnier F, Alberti C, Artigas A, Teres D. The Logistic Organ Dysfunction system. A new way to assess organ dysfunction in the intensive care unit. ICU Scoring Group. *JAMA* 1996;276:802–810.
26. Vincent JL, Moreno R, Takala J, Willatts S, De Mendonça A, Bruining H, Reinhart CK, Suter PM, Thijs LG. The SOFA (Sepsis-related Organ Failure Assessment) score to describe organ dysfunction/failure. On behalf of the Working Group on Sepsis-Related Problems of the European Society of Intensive Care Medicine. *Intensive Care Med* 1996. pp. 707–710.
27. Camus C, Salomon S, Bouchigny C, Gacouin A, Lavoué S, Donnio P-Y, Javaudin L, Chaplain J-M, Le Tulzo Y, Bellissant E. Short-Term Decline in All-Cause Acquired Infections With the Routine Use of a Decontamination Regimen Combining Topical Polymyxin, Tobramycin, and Amphotericin B With Mupirocin and Chlorhexidine in the ICU. *Crit Care Med* 2014;42:1121–1130.
28. Roussel M, Benard C, Ly-Sunnaram B, Fest T. Refining the white blood cell differential: The first flow cytometry routine application. *Cytometry* 2010;77A:552–563.
29. Ziegler-Heitbrock L, Ancuta P, Crowe S, Dalod M, Grau V, Hart DN, Leenen PJM, Liu YJ, MacPherson G, Randolph GJ, Scherberich J, Schmitz J, Shortman K, Sozzani S, Strobl H, Zembala M, Austyn JM, Lutz MB. Nomenclature of monocytes and dendritic cells in blood. *Blood* 2010;116:e74–e80.
30. Loï C, Zazzo J-F, Delpierre E, Niddam C, Neveux N, Curis E, Arnaud-Battandier F, Cynober L. Increasing plasma glutamine in postoperative patients fed an arginine-rich immune-enhancing diet—A pharmacokinetic randomized controlled study\*. *Crit Care Med* 2009;37:501–509.
31. Eisen MB, Spellman PT, Brown PO, Botstein D. Cluster analysis and display of genome-wide expression patterns. *Proc Natl Acad Sci USA* 1998;95:14863–14868.
32. Scicluna BP, Klein Klouwenberg PMC, van Vught LA, Wiewel MA, Ong DSY, Zwinderman AH, Franitza M, Toliat MR, Nürnberg P, Hoogendijk AJ, Horn J, Cremer OL, Schultz MJ, Bonten MJ, van der Poll T. A Molecular Biomarker to Diagnose Community-acquired Pneumonia on Intensive Care Unit Admission. *Am J Respir Crit Care Med* 2015;192:826–835.
33. Poehlmann H, Schefold JC, Zuckermann-Becker H, Volk H-D, Meisel C. Phenotype changes and impaired function of dendritic cell subsets in patients with sepsis: a prospective observational analysis. *Crit Care* 2009;13:R119.
34. Brandau S, Moses K, Lang S. The kinship of neutrophils and granulocytic myeloid-derived suppressor cells in cancer: cousins, siblings or twins? *Seminars in Cancer Biology* 2013;23:171–182.
35. Sinha P, Okoro C, Foell D, Freeze HH, Ostrand-Rosenberg S, Srikrishna G. Proinflammatory S100 Proteins Regulate the Accumulation of Myeloid-Derived Suppressor Cells. *J Immunol* 2008;181:4666–4675.
36. Waight JD, Hu Q, Miller A, Liu S, Abrams SI. Tumor-Derived G-CSF Facilitates Neoplastic Growth through a Granulocytic Myeloid-Derived Suppressor Cell-

- Dependent Mechanism. In: Blagosklonny MV, editor. *PLoS ONE* 2011;6:e27690–15.
37. Munder M. Arginase I is constitutively expressed in human granulocytes and participates in fungicidal activity. *Blood* 2005;105:2549–2556.
  38. Faurschou M, Borregaard N. Neutrophil granules and secretory vesicles in inflammation. *Microbes and Infection* 2003;5:1317–1327.
  39. Boomer JS, To K, Chang KC, Takasu O, Osborne DF, Walton AH, Bricker TL, Jarman SD, Kreisel D, Krupnick AS, Srivastava A, Swanson PE, Green JM, Hotchkiss RS. Immunosuppression in patients who die of sepsis and multiple organ failure. *JAMA* 2011;306:2594–2605.
  40. Drewry AM, Samra N, Skrupky LP, Fuller BM, Compton SM, Hotchkiss RS. Persistent Lymphopenia After Diagnosis of Sepsis Predicts Mortality. *Shock* 2014;42:383–391.
  41. Monneret G, Finck M-E, Venet F, Debard A-L, Bohé J, Bienvenu J, Lepape A. The anti-inflammatory response dominates after septic shock: association of low monocyte HLA-DR expression and high interleukin-10 concentration. *Immunology Letters* 2004;95:193–198.
  42. Cavaillon J-M, Adib-Conquy M. Bench-to-bedside review: endotoxin tolerance as a model of leukocyte reprogramming in sepsis. *Crit Care* 2006;10:233.
  43. Monneret G, Lepape A, Voirin N, Bohé J, Venet F, Debard A-L, Thizy H, Bienvenu J, Gueyffier F, Vanhems P. Persisting low monocyte human leukocyte antigen-DR expression predicts mortality in septic shock. *Intensive Care Med* 2006;32:1175–1183.
  44. Zhang K, Bai X, Li R, Xiao Z, Chen J, Yang F, Li Z. Endogenous glucocorticoids promote the expansion of myeloid-derived suppressor cells in a murine model of trauma. *Int J Mol Med* 2012;30:277–282.
  45. Kovach MA, Standiford TJ. The function of neutrophils in sepsis. *Current Opinion in Infectious Diseases* 2012;25:321–327.
  46. Mathias B, Delmas AL, Ozrazgat-Baslanti T, Vanzant EL, Szpila BE, Mohr AM, Moore FA, Brakenridge SC, Brumback BA, Moldawer LL, Efron PA. Human Myeloid-derived Suppressor Cells are Associated With Chronic Immune Suppression After Severe Sepsis/Septic Shock. *Ann Surg* 2016;[Epub ahead of print].doi:10.1097/SLA.0000000000001783.
  47. Cuenca AG, Delano MJ, Kelly-Scumpia KM, Moreno C, Scumpia PO, Laface DM, Heyworth PG, Efron PA, Moldawer LL. A paradoxical role for myeloid-derived suppressor cells in sepsis and trauma. *Mol Med* 2011;17:281–292.
  48. Brudecki L, Ferguson DA, McCall CE, Gazzar El M. Myeloid-Derived Suppressor Cells Evolve during Sepsis and Can Enhance or Attenuate the Systemic Inflammatory Response. In: Bäumlér AJ, editor. *Infect Immun* 2012;80:2026–2034.
  49. Rodriguez PC, Ernstoff MS, Hernandez C, Atkins M, Zabaleta J, Sierra R, Ochoa AC. Arginase I-Producing Myeloid-Derived Suppressor Cells in Renal Cell Carcinoma Are a Subpopulation of Activated Granulocytes. *Cancer*

*Research* 2009;69:1553–1560.

50. Cloke T, Munder M, Taylor G, Müller I, Kropf P. Characterization of a Novel Population of Low-Density Granulocytes Associated with Disease Severity in HIV-1 Infection. In: Boasso A, editor. *PLoS ONE* 2012;7:e48939.
51. Sagiv JY, Michaeli J, Assi S, Mishalian I, Kisos H, Levy L, Damti P, Lumbroso D, Polyansky L, Sionov RV, Ariel A, Hovav A-H, Henke E, Fridlender ZG, Granot Z. Phenotypic Diversity and Plasticity in Circulating Neutrophil Subpopulations in Cancer. *CellReports* 2015;10:562–573.
52. Popovic PJ, Zeh HJ, Ochoa JB. Arginine and immunity. *The Journal of nutrition* 2007;
53. Taneja R, Parodo J, Jia SH, Kapus A, Rotstein OD, Marshall JC. Delayed neutrophil apoptosis in sepsis is associated with maintenance of mitochondrial transmembrane potential and reduced caspase-9 activity\*. *Crit Care Med* 2004;32:1460–1469.
54. Drifte G, Dunn-Siegrist I, Tissières P, Pugin J. Innate Immune Functions of Immature Neutrophils in Patients With Sepsis and Severe Systemic Inflammatory Response Syndrome\*. *Crit Care Med* 2013;41:820–832.
55. van Vught LA, Klein Klouwenberg PMC, Spitoni C, Scicluna BP, Wiewel MA, Horn J, Schultz MJ, Nürnberg P, Bonten MJM, Cremer OL, van der Poll T, MARS Consortium. Incidence, Risk Factors, and Attributable Mortality of Secondary Infections in the Intensive Care Unit After Admission for Sepsis. *JAMA* 2016;315:1469–1479.
56. Xu J, Escamilla J, Mok S, David J, Priceman S, West B, Bollag G, McBride W, Wu L. CSF1R Signaling Blockade Stanches Tumor-Infiltrating Myeloid Cells and Improves the Efficacy of Radiotherapy in Prostate Cancer. *Cancer Research* 2013;73:2782–2794.
57. Qin H, Lerman B, Sakamaki I, Wei G, Cha SC, Rao SS, Qian J, Hailemichael Y, Nurieva R, Dwyer KC, Roth J, Yi Q, Overwijk WW, Kwak LW. Generation of a new therapeutic peptide that depletes myeloid-derived suppressor cells in tumor-bearing mice. *Nature Medicine* 2014;1–8.doi:10.1038/nm.3560.
58. Lai D, Qin C, Shu Q. Myeloid-derived suppressor cells in sepsis. *Biomed Res Int* 2014;2014:598654.

## FIGURE LEGENDS

### ***Figure 1: Peripheral blood transcriptomic analysis reveals a myeloid suppressive signature in septic patients.***

(A) Hierarchical clustering of 44 immune-related genes, in septic patients and healthy donors (HD). The level of expression of each gene was determined on whole blood RNA by qRT-PCR (TLDA) in 15 HD and 29 septic patients, and analyzed by unsupervised hierarchical clustering with Spearman's rank distance and average linkage. Color intensity is related to the expression fold change; red = increased expression, green = decreased expression, black = no significant variation.

(B) Gene set enrichment analysis (GSEA) plot for upregulated genes involved in MDSC signature (*Table 1*) on a published cohort of septic patients (GSE65682).

(C) Correlation between gene expression and lymphocyte or granulocyte counts.

(D) Ratio of *CD247* (CD3ζ) to *CD3G* (CD3γ) peripheral blood expression and correlation with granulocyte count. Box = interquartile range and median, whiskers = range, points = outlying values; comparisons between groups were performed using Mann-Whitney *U* test. Spearman's rank correlation coefficients ( $\rho$ ) and *p* values are indicated for each correlation. \*\*  $p < .01$ .

### ***Figure 2: Peripheral blood myeloid cells display a suppressive phenotype in septic patients.***

(A) Myeloid cell subsets in septic patients (sepsis) and healthy donors (HD). Whole blood monocyte subset counts were determined by flow cytometry in 36 septic patients and 26 healthy donors. Mature and immature granulocytic subset counts were determined on white blood cell differentials by flow cytometry in 88 septic

patients and 44 healthy donors. The proportion of low-density granulocytes (LDGs) among PBMCs is shown for 88 septic patients and 16 healthy donors. The absolute peripheral LDG count is inferred from the ratio of LDGs to CD3<sup>pos</sup> lymphocytes among PBMCs and the absolute CD3<sup>pos</sup> lymphocyte count. Spearman's rank correlation coefficients (rho) and p values are indicated for each correlation.

(B) CD14<sup>pos</sup>HLA-DR<sup>lo/neg</sup> monocyte and LDG counts were compared to values obtained in 11 intensive care unit non-septic patients (ICU). Kruskal Wallis with Dunn's multiple comparisons test.

(C) Inducers and mediators of MDSC activity in septic patients and healthy donors (HD). Plasma levels of S100A8/A9, S100A12 proteins and arginase 1 enzyme were determined by ELISA in 16 healthy donors and 73 septic patients. Plasma levels of G-CSF were determined by ELISA in 10 healthy donors and 25 septic patients. Plasma concentration of Arginine (19 healthy donors, 73 sepsis) and kynurenine / tryptophan ratio (19 healthy donors, 21 sepsis) were measured by high-performance liquid chromatography. Box = interquartile range and median, whiskers = range, points = outlying values; comparisons between groups were performed using Mann-Whitney *U* test; \* p<.05, \*\* p<.01, \*\*\* p<.001, \*\*\*\* p<.0001; ns, non significant.

***Figure 3: CD14<sup>pos</sup> monocytes and CD15<sup>pos</sup> low-density granulocytes display a myeloid-derived suppressor cell activity in septic patients.***

(A) T-cell proliferation is deeply impaired in septic patients. Fresh PBMCs obtained from septic patients (n=10) or healthy donors (HD, n=8) were stimulated with anti-CD3/anti-CD28 antibodies after CFSE labeling. The proportions of CD4<sup>pos</sup> and CD8<sup>pos</sup> proliferated T-cells ( $\geq$  G2 generation) were determined at day 4 by flow

cytometry. Box = interquartile range and median, whiskers = range, points = outlying values; comparisons between groups were performed using Mann-Whitney *U* test. \*\*  $p < .01$ , \*\*\*\*  $p < .0001$ .

(B) CD14<sup>pos</sup> monocytes and CD15<sup>pos</sup> low-density granulocytes (LDGs) suppress *in vitro* T-cell proliferation in septic patients. Fresh PBMCs obtained from septic patients or healthy donors (HD) were depleted of CD14<sup>pos</sup> monocytes (PBMC-CD14<sup>pos</sup> cells), of CD15<sup>pos</sup> LDGs (PBMC-CD15<sup>pos</sup> cells), or not depleted (PBMC), and stimulated with anti-CD3/anti-CD28 antibodies after CFSE labeling. The proportion of CD4<sup>pos</sup> and CD8<sup>pos</sup> proliferated T-cells ( $\geq$  G2 generation) was determined at day 4 by flow cytometry. Dashed lines represent the median of healthy donor values (n=8), points and lines represent paired values for septic patients. Proliferation values with or without depletion were compared using the Wilcoxon matched-pairs signed rank test. \*  $p < .05$ , \*\*  $p < .01$ .

(C) LDGs are responsible for an arginase activity *in vitro*. The concentrations of arginine and ornithine were determined by high-performance liquid chromatography in the supernatants of PBMCs depleted or not of CD14<sup>pos</sup> or CD15<sup>pos</sup> cells. Friedman with Dunn's multiple comparisons test between depleted and not-depleted PBMCs; \*\*  $p < .01$ . Spearman's rank correlation coefficient ( $\rho$ ) and *p* value is indicated for each correlation.

***Figure 4: High initial levels of granulocytic myeloid-derived suppressor cells predict occurrence of nosocomial infections.***

(A) High initial proportion of low-density granulocytes (LDGs) and elevated immature neutrophil count predict the development of nosocomial infections. The mature and

immature granulocytic subset counts on a white blood cells differential and the proportion of low-density granulocytes (LDGs) among PBMCs were determined by flow cytometry in 88 septic patients, of which 21 (22%) developed nosocomial infection(s) (NI). The Kaplan-Meier curve represents the cumulative incidence of nosocomial infections according to initial G-MDSC proportion. Grey line, MDSC < 36% of PBMCs; Dark line, G-MDSCs > 36% of PBMCs. Censored subject (vertical hash marks) represent patients who were either discharged from the hospital or who died without events.

(B) Whole blood CD14<sup>pos</sup>HLA-DR<sup>low/neg</sup> (M-MDSC) count was determined by flow cytometry in 36 patients. Among them, 9 (25%) developed nosocomial infection(s).

(C) Plasma levels of S100A12 protein were determined by ELISA in 73 patients, 18 (24,7%) of which developed nosocomial infection(s). Plasma levels of G-CSF and arginase 1 enzyme were respectively determined by multiplex Luminex assay and ELISA in 26 patients. Among them, 6 (23,1%) developed nosocomial infection(s). Box = interquartile range and median, whiskers = range, points = outlying values; comparisons between groups were performed using Mann-Whitney *U* test. The Mantel-Cox log-rank test was used to compare the Kaplan-Meier curves. \*  $p < .05$ ; \*\*  $p < .01$ ; ns, non-significant.

**Figure 5: Characterization of low-density granulocytes in septic patients.**

(A) Low-density granulocytes (LDGs) are enriched for immature cells compared to high-density granulocytes (HDGs). The proportion of mature CD11b<sup>pos</sup>CD16<sup>high</sup> polymorphonuclear cells (PMN), immature CD11b<sup>pos</sup>CD16<sup>low</sup> metamyelocytes (MM), CD11b<sup>pos</sup>CD16<sup>neg</sup> myelocytes (M) and CD11b<sup>neg</sup>CD16<sup>neg</sup> promyelocytes (PM) in the

LDGs versus HDGs fractions in septic patients were determined by flow cytometry after Ficoll density centrifugation. Error bars represent  $\pm$ SEM. \*\*p <.01. The proportions of granulocyte subsets between LDGs and HDGs were compared with Wilcoxon matched-pairs signed rank test; \*\* p<.01.

(B) HDGs are a homogeneous population of mature neutrophils, whereas LDGs are composed of neutrophils at different stages of maturation, including mature segmented neutrophils as well as more immature banded neutrophils and myelocytes. May-Grünwald-Giemsa-stained cytopsin slides of purified CD15<sup>pos</sup> cells from density gradient interface (LDGs) and pellet (HDGs).

(C) LDGs express higher levels of genes involved in the granulocytic maturation. Gene expression was evaluated by qPCR on paired LDGs and HDGs purified from 5 septic patients. For each gene, the relative expression (mRNA  $2^{-\Delta\Delta C_t}$ ) in paired LDGs and HDGs was compared (ratio of the mean expression in LDGs to the mean expression in HDGs).

(D, E) LDGs express high levels of degranulation markers. Mean fluorescence intensity (MFI) of degranulation surface markers (CD35, CD63, CD66b), size (forward scatter, FS) and granularity (SS, side scatter) were compared by flow cytometry between LDGs and HDGs purified from 9 septic patients. Box = interquartile range and median, whiskers = range, points = outlying values; Wilcoxon matched-pairs signed rank test; \* p<.05, \*\* p<.01.

(F) Plasma levels of neutrophil granule proteins are increased in septic patients. Plasma levels of myeloperoxidase (MPO) and neutrophil gelatinase-associated lipocalin (NGAL) were determined by ELISA in 16 healthy donors (HD) and 74 septic

patients. Box = interquartile range and median, whiskers = range, points = outlying values; Mann-Whitney  $U$  test; \*\*\*\*  $p < .0001$ .

TABLES

**Table 1. Differentially expressed genes in the peripheral blood from septic patients and healthy donors.**

	Gene Name	Fold change	p	FDR
UPREGULATED	MMP8	25.76	< .0001	< .0002
	ARG1	22.48	< .0001	< .0002
	S100A12	21.40	< .0001	< .0002
	SLPI	9.80	< .0001	< .0002
	S100A9	8.49	< .0001	< .0002
	MMP9	7.02	< .0001	< .0002
	IL10	6.85	< .0001	< .0002
	ELANE	6.36	.0002	.0003
	TNFAIP6	5.52	< .0001	< .0002
	AIM2	5.21	< .0001	< .0002
	CD274	4.55	.0003	.0004
	S100A8	3.14	.0038	.0042
	FKBP5	2.96	< .0001	< .0002
	IL4R	2.27	< .0001	< .0002
	PGF	2.09	.0038	.0042
	MYD88	2.07	< .0001	< .0002
	ADAM17	1.95	< .0001	< .0002
	FUT4	1.41	.0013	.0016
	CASP1	1.36	.0041	.0044
DOWNREGULATED	CCL2	.09	< .0001	< .0002
	CD247	.16	< .0001	< .0002
	IL4	.22	< .0001	< .0002
	NCR1	.23	.0001	.0002
	CD4	.24	< .0001	< .0002
	MS4A1	.24	.0001	.0002
	FLT3LG	.25	< .0001	< .0002
	CD8B	.27	< .0001	< .0002
	CD3G	.27	< .0001	< .0002
	IL8	.32	.0001	.0002
	CSF1R	.34	.0005	.0007
	IL6	.42	.0023	.0027
	NLRP1	.47	< .0001	< .0002
	NOS2	.49	.0142	.0142
	KITLG	.51	.0023	.0027
	IL12A	.72	.0108	.0111

Fold changes represent medians of the  $2^{-\Delta\Delta C_t}$  values. Two-tailed Mann-Whitney *U*-test. FDR represent false discovery rate adjusted p-values.

**Table 2. Characteristics of patients and healthy donors.**

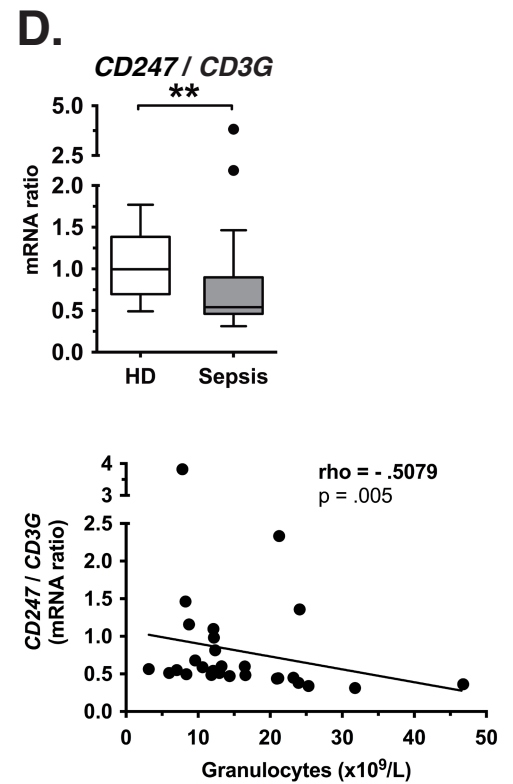
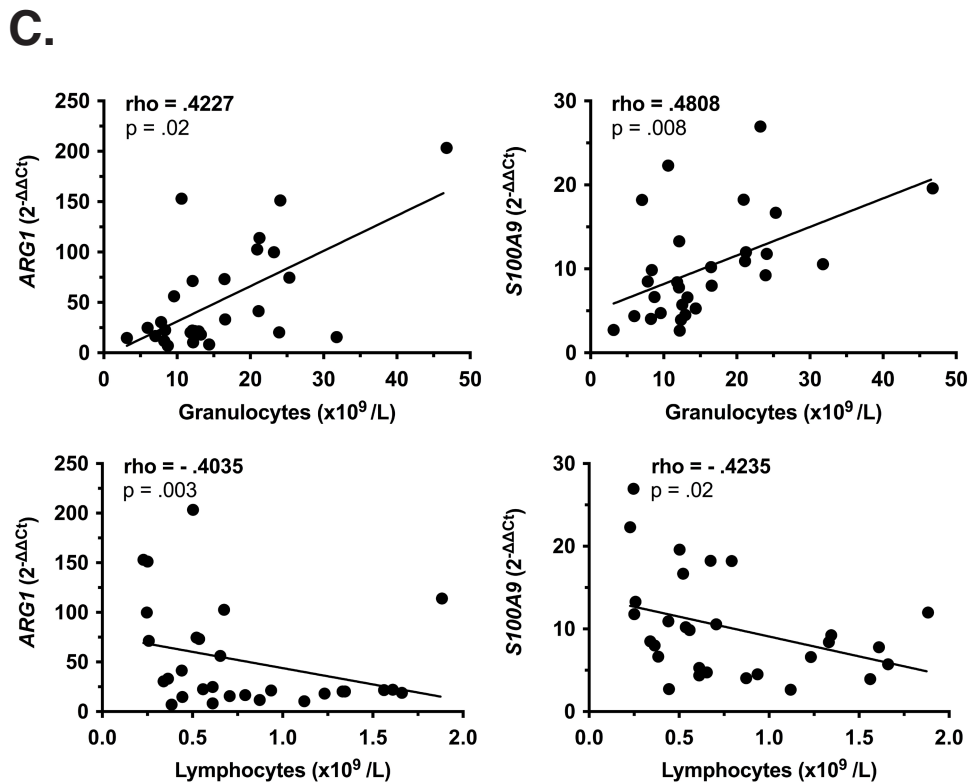
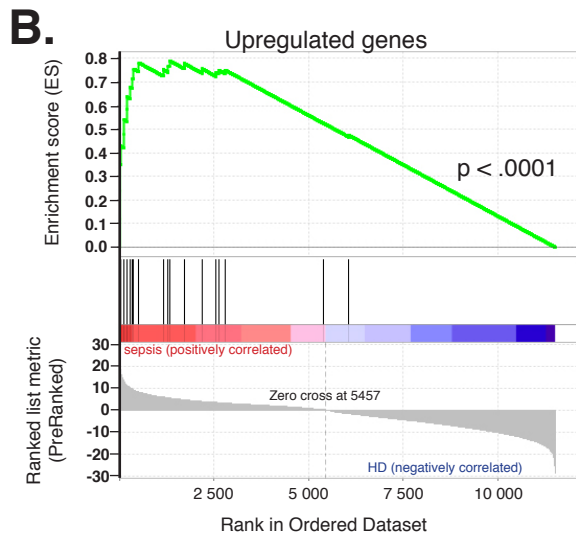
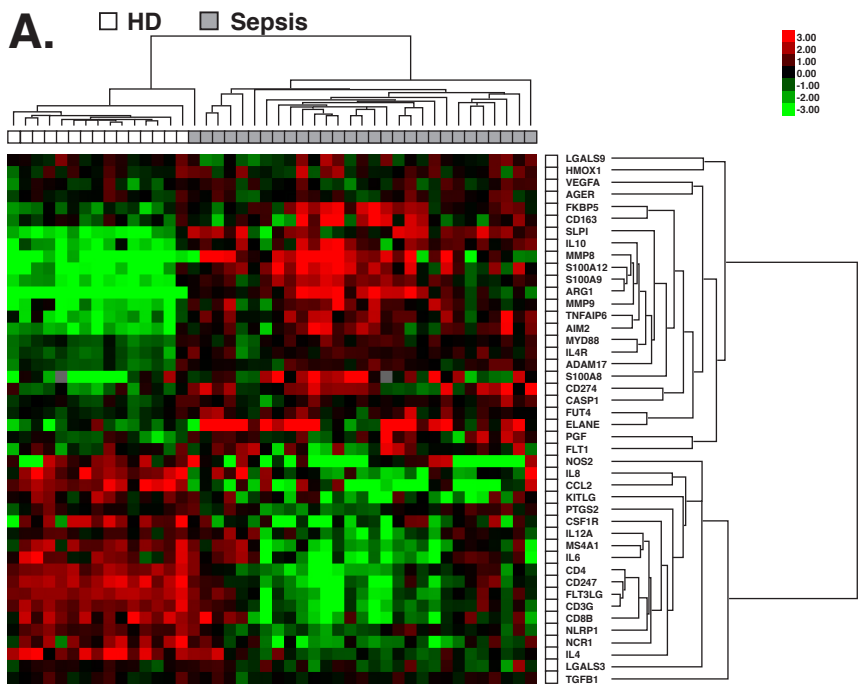
Characteristics	ICU Patients			Healthy donors (n = 67)
	Septic shock (n = 72)	Severe sepsis (n = 22)	ICU non-septic* (n=11)	
Male sex, n (%)	42 (58%)	14 (64%)	8 (72%)	41 (61%)
Age, years	63 [53-73]	57 [41-75]	70 [62-76]	56 [49-60]
ICU length of stay, days	10 [4-18]	4 [2-7]	7 [5-16]	NA
Hospital length of stay, days	26 [13-47]	19 [7-23]	10,5 [6-17]	NA
Total duration of MV, days	6 [1-15]	0 [0-4]	7 [4-13]	NA
Died / Survived	18/54	1/21	6/5	NA
SAPS II	51 [38-63]	30 [22-40]	47 [41-83]	NA
SOFA	10 [8-13]	4 [2-6]	9 [6-13]	NA
Organ dysfunctions	3 [2-4]	1 [0-2]	3 [3-3]	NA
LOD score	6 [3-9]	3 [0-4]	8 [5-9]	NA

Data are expressed as median [interquartile range] unless otherwise indicated. ICU, intensive care unit; LOD, Logistic Organ Dysfunction; MV, Mechanical ventilation; NA, Not applicable; SAPS, Simplified Acute Physiology Score; SOFA, Sepsis-related Organ Failure Assessment.

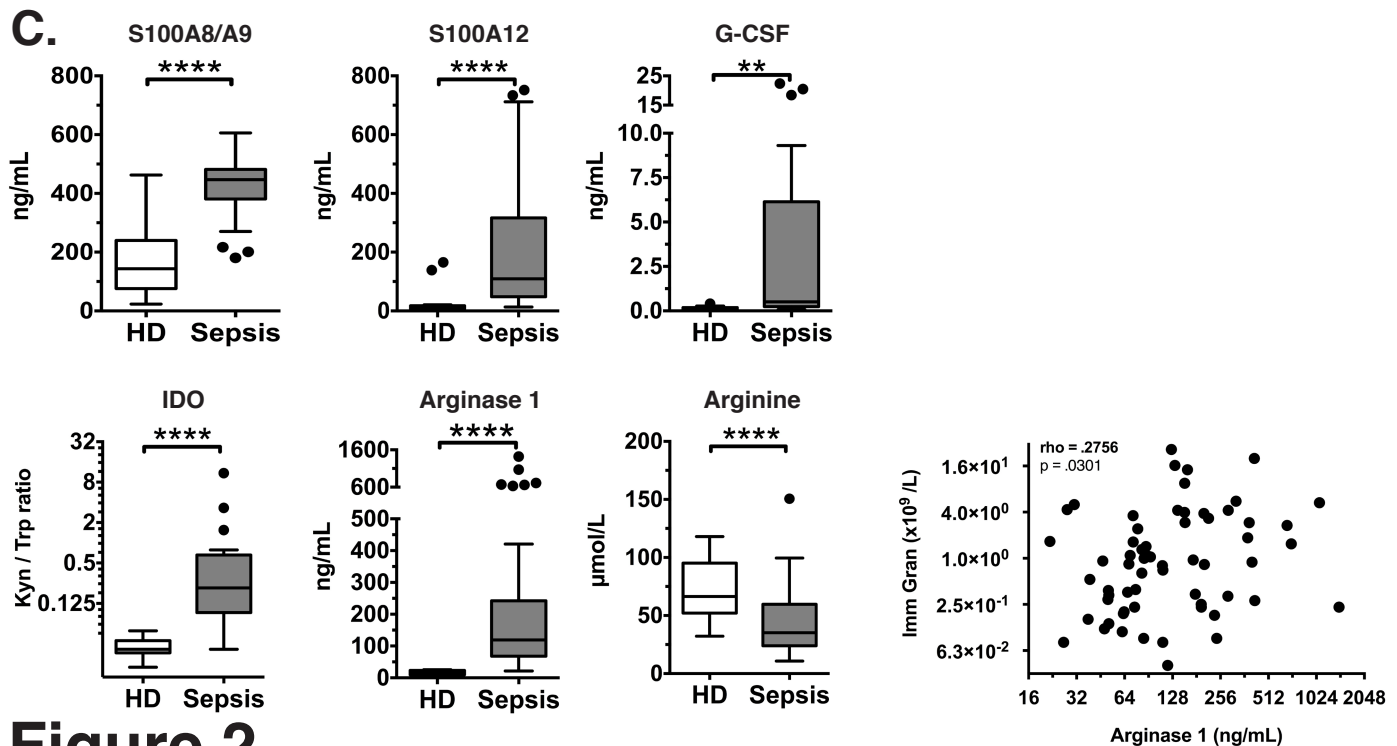
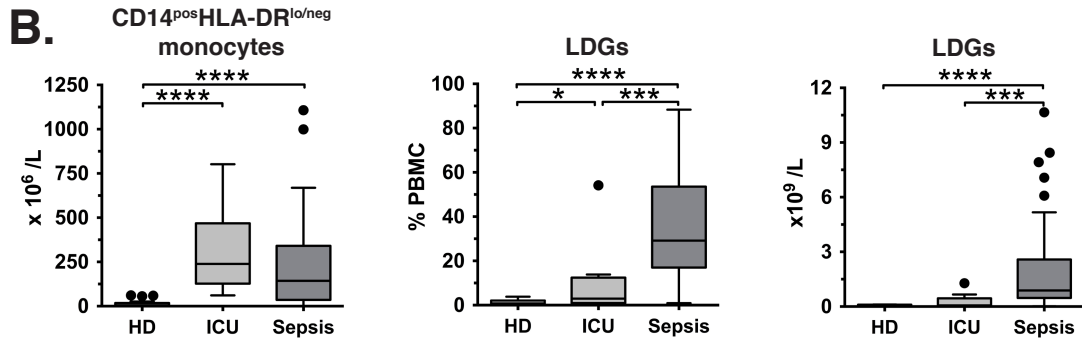
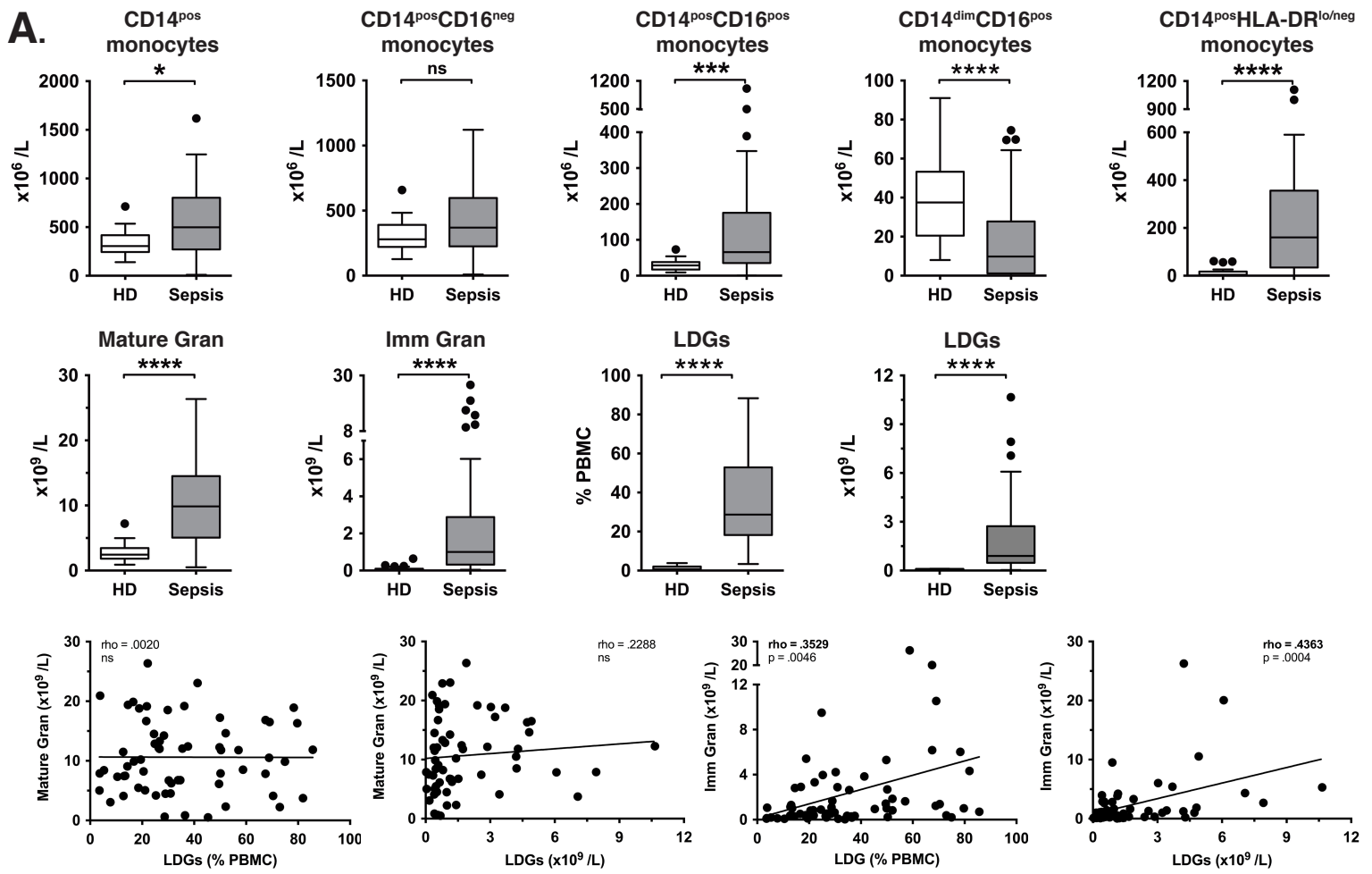
\* Cardiac arrest (n=6), acute heart failure (n=4), Ischemic stroke (n=1).

**Table 3. Sites of infection and microorganisms isolated in septic patients.**

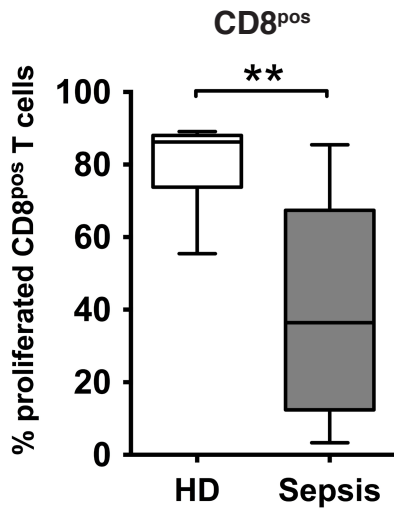
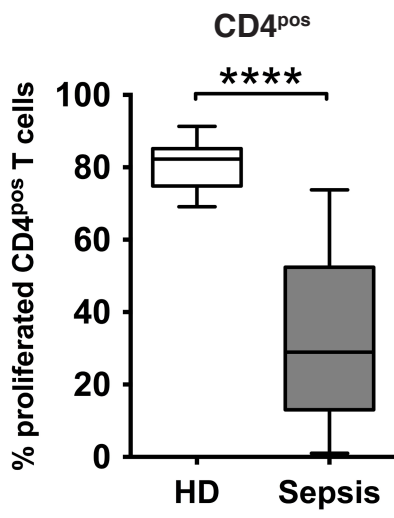
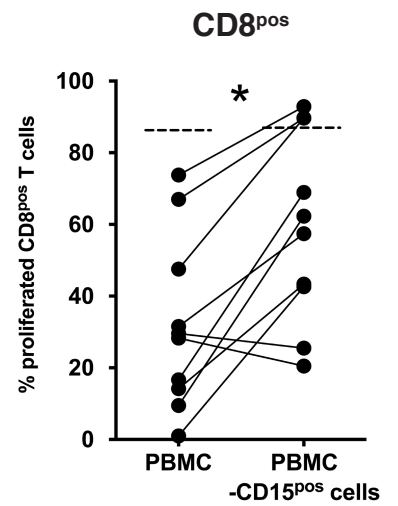
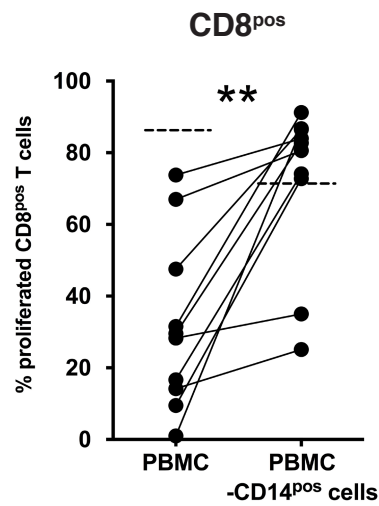
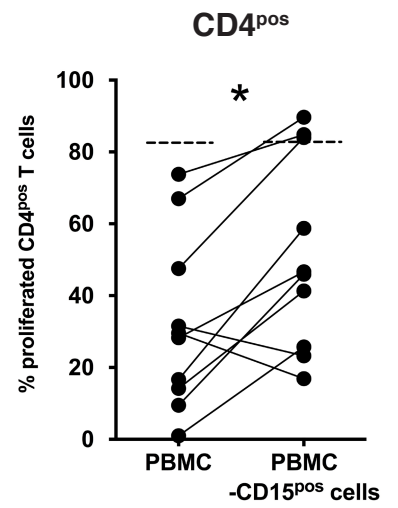
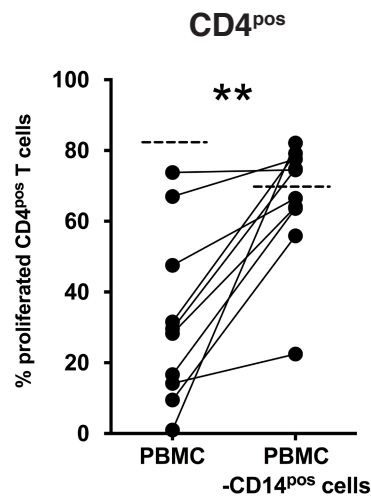
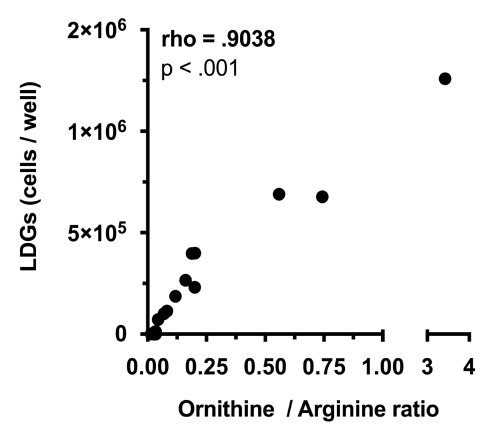
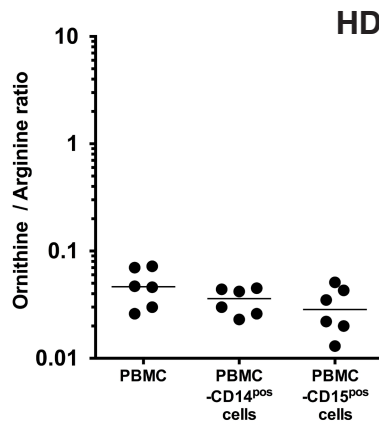
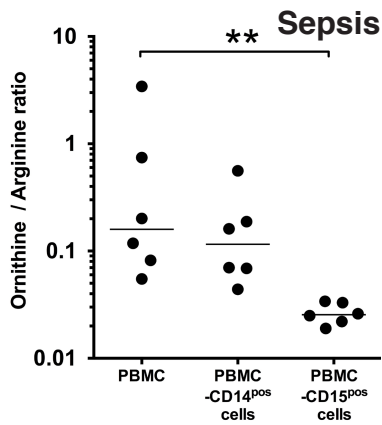
Characteristics	Septic shock (n = 72)	Severe sepsis (n = 22)
Infection site, no. of patients		
Respiratory tract	23	8
Intra-abdominal/pelvis	11	1
Urinary tract	8	5
Vascular	7	2
Central nervous system	3	3
Other sources	19	3
Unknown	1	0
Bacteremia	39	11
Isolates, no. of patients		
Gram positive	37	9
Gram negative	18	9
Miscellaneous	5	0
Candida	1	0
Unknown	11	4

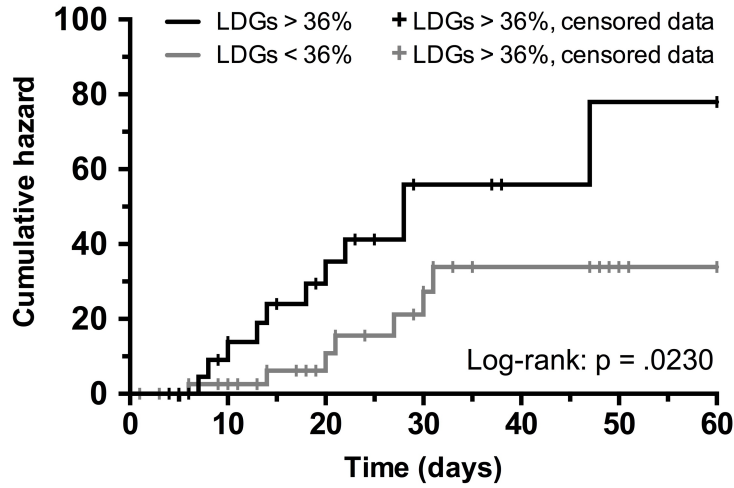
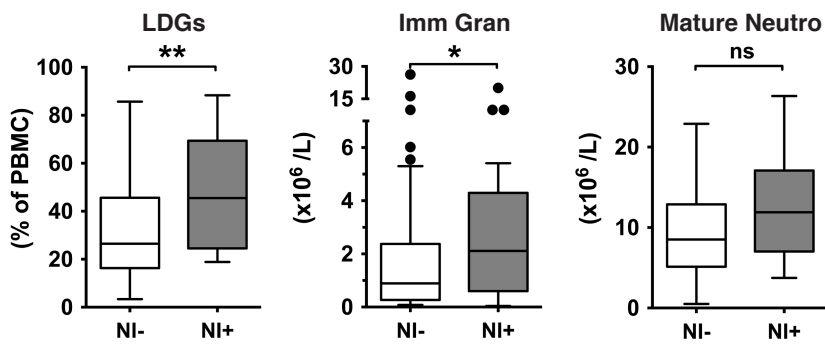


**Figure 1**



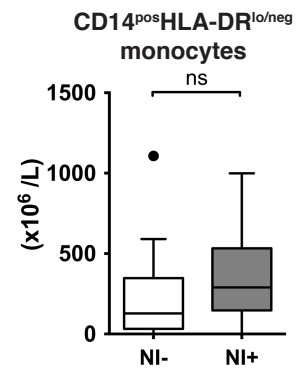
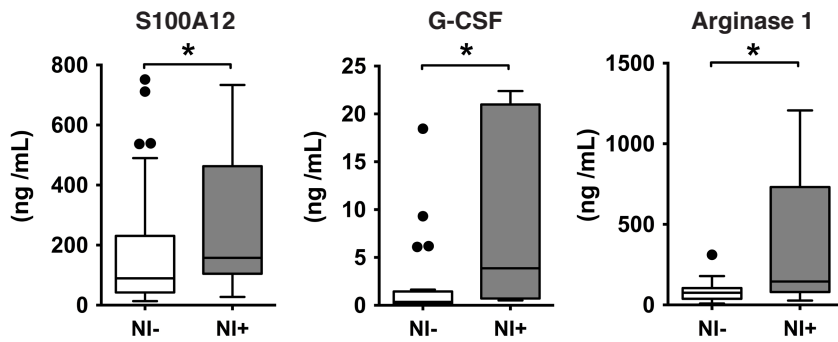
**Figure 2**

**A.****B.****C.****Figure 3**

**A.**

Numbers at risk

LDGs < 36%	45	33	20	13	8	3	1
LDGs > 36%	26	19	12	6	3	2	1

**B.****C.****Figure 4**

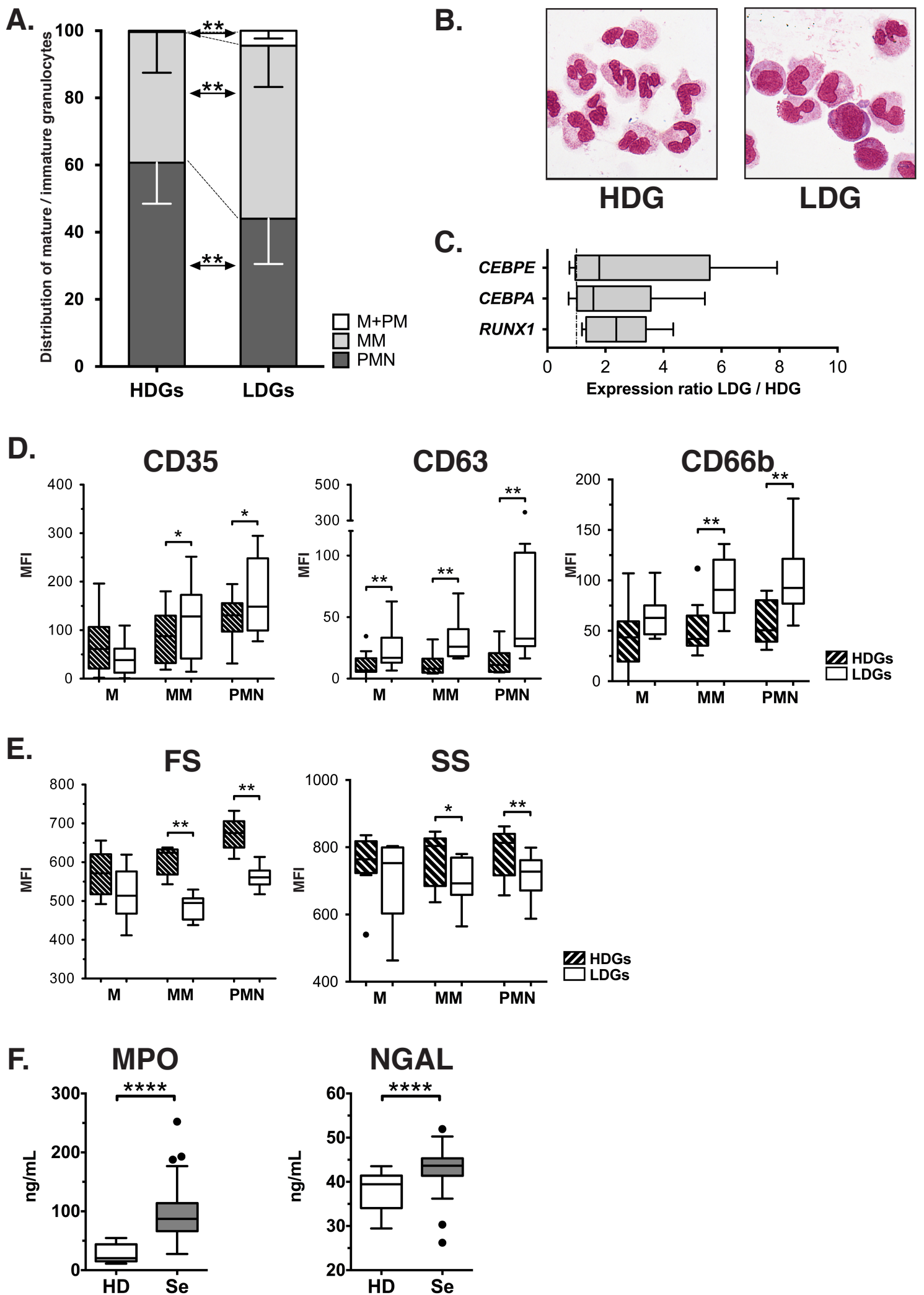


**Figure 5**

# Online data supplement

## **Early expansion of circulating myeloid-derived suppressor cells predicts development of nosocomial infections in septic patients.**

Fabrice Uhel, MD, PhD<sup>1,2,3</sup>, Imane Azzaoui, PhD<sup>3,4,5,6</sup>, Murielle Grégoire, PhD<sup>3,4,5,6</sup>, Céline Pangault, PharmD, PhD<sup>3,4,5,6</sup>, Joelle Dulong, MBiol<sup>3,4,5,6</sup>, Jean-Marc Tadié, MD, PhD<sup>1,2,3,5</sup>, Arnaud Gacouin, MD<sup>1,2</sup>, Christophe Camus, MD, PhD<sup>1,2</sup>, Luc Cynober, PharmD, PhD<sup>7</sup>, Thierry Fest, MD, PhD<sup>3,4,5,6</sup>, Yves Le Tulzo, MD, PhD<sup>1,2,3,5</sup>, Mikael Roussel, MD, PhD<sup>3,4,5,6</sup> and Karin Tarte, Pharm D, PhD<sup>3,4,5,6</sup>

## SUPPLEMENTAL METHODS

### *Quantitative real-time PCR*

Total RNA was extracted using PAXgene blood RNA kit (Qiagen). cDNA was then generated using Multiscribe Reverse Transcriptase and High-Capacity cDNA reverse Transcription kit (Invitrogen). For quantitative RT-PCR on whole blood, we used Taqman array microfluidic cards and Taqman Universal Master Mix from Applied Biosystems (Invitrogen). A panel of genes related to myeloid suppressor cells was selected based on literature knowledge. Gene expression was measured by the ABI Prism 7900HT Sequence Detection System. *18S*, *CDKN1B* and *ELF1* were determined as appropriate internal standards using TaqMan endogenous control assays (Invitrogen) and geNorm algorithm analysis (<https://genorm.cmgg.be>). For each sample, the gene CT values were determined, normalized to the geometric mean value of the 3 housekeeping genes, and compared to the median value obtained from healthy donors using the  $2^{-\Delta\Delta CT}$  method.

Quantitative RT-PCR were also performed on purified low- (LDG) and high-density granulocytes (HDG) from 5 septic patients. cDNA was prepared using Fluidigm Reverse Transcription Master Mix (Fluidigm, Sunnyvale, CA). The qPCR was performed in triplicate using 96.96 Dynamic Array integrated fluidics circuit and the BioMark HD System from Fluidigm. *CDKN1B* and *PUM1* were determined as appropriate internal standards using TaqMan endogenous control assays (Invitrogen) and geNorm algorithm analysis (<https://genorm.cmgg.be>). For each LDG sample, the mean Ct value for the gene of interest was calculated, normalized to the geometric mean value of housekeeping genes, and compared with value obtained from the paired HDG samples using the  $2^{-\Delta\Delta Ct}$  method. For each gene, results were expressed as the ratio of paired LDG to HDG  $2^{-\Delta\Delta Ct}$  values.

### *Cell isolation and culture*

Fresh PBMCs were obtained from healthy donors or septic patients after Ficoll density centrifugation. Cells were magnetically depleted or not for monocytes or LDGs using CD14 or CD15 microbeads (Miltenyi Biotec). Purity and viability after depletion evaluated by flow cytometry were always >97%. Purified cells were labeled with carboxyfluorescein succinimidyl ester (CFSE; Interchim) and cultured in 96-well round-bottom plates with RPMI 1640-10% human AB serum (Biowest) in the presence of anti-CD3 and anti-CD28 monoclonal antibodies (0.6 µg/mL, Sanquin). After 4 days, cells were labeled with anti-CD2, anti-CD4, and anti-CD8 monoclonal antibodies (Table E1) and resuspended in DAPI buffer to

identify viable cells. CFSE dilution was assessed by flow cytometry. Results were analyzed with ModFit LT software (Verity Software House) and expressed as the cumulated proportion of proliferated T-cells ( $\geq$  G2 generation).

**SUPPLEMENTAL TABLES**

**Table E1. Antibodies used for flow cytometry**

<b>Cell sample</b>	<b>Panel</b>	<b>Reactivity</b>	<b>Conjugate</b>	<b>Supplier</b>
<b>Whole blood</b>	Cytodiff Panel	CD36	FITC	Beckman Coulter
		CD2 + CD294	PE	
		CD19	ECD	
		CD16	PC5	
		CD45	PC7	
	DC	Lin 1	FITC	BD Biosciences
		CD141	PE	Miltenyi Biotech
		HLA-DR	ECD	Beckman Coulter
		CD123	PerCP-Cy5.5	BD Biosciences
		CD11b	PC7	Beckman Coulter
		CD1c	APC	Miltenyi Biotech
		CD11c	Alexa 700	BD Biosciences
		CD33	APC-Alexa 750	Beckman Coulter
		CD34	VioBlue	Miltenyi Biotech
		CD45	Krome Orange	Beckman Coulter
	Mono / M-MDSC	HLA-DR	PE-CF594	BD Biosciences
		CD115	PerCP 5.5	BD Biosciences
		CD14	PC7	Beckman Coulter
		CCR2	A647	BD Biosciences
		CD16	APC-Alexa 700	Beckman Coulter
		CD64	APC-Alexa 750	Beckman Coulter
		CD3	V450	BD Biosciences
		CD335	BV421	BioLegend
		CD45	Krome Orange	Beckman Coulter
	mHLA-DR	HLA-DR	FITC	Beckman Coulter
		IgG1	FITC	Beckman Coulter
		CD14	PC7	Beckman Coulter
PBMC / G-MDSC	CD14	PE	Beckman Coulter	
	HLA-DR	PE-CF594	BD Biosciences	
	CD3	PC7	Beckman Coulter	
	CD16	APC-Alexa 700	Beckman Coulter	
	CD15	Pacific Blue	Beckman Coulter	
	CD45	Krome Orange	Beckman Coulter	
PBMC	CD66b	FITC	Beckman Coulter	
	CD35	PE	BD Biosciences	
	CD11b	PerCP 5.5	BD Biosciences	
	CD63	PC7	BD Biosciences	
	CD16	APC-Alexa 700	Beckman Coulter	
	CD15	Pacific Blue	Beckman Coulter	
	CD45	Krome Orange	Beckman Coulter	
T-cell Proliferation	CD2	PC7	Beckman Coulter	
	CD4	Alexa 700	BD Biosciences	
	CD8	APC	Beckman Coulter	

**Table E2. Description of nosocomial infections**

Site	n=
Nosocomial pneumonia	7
Urinary tract infection	4
Central venous catheter-related infection	2
Spontaneous bacteremia	2
Skin and soft tissues infections	2
Gastrointestinal system infections	3
Cardiovascular system infection	1

## SUPPLEMENTAL FIGURE LEGENDS

### **Figure E1. Gating strategy for myeloid cells subpopulations, monocytic- and granulocytic-myeloid-derived suppressor cells.**

(A) Definition of dendritic cells subsets. Peripheral blood from healthy donors or septic patients was stained for Lin 1 (lineage 1, CD3/CD14/CD19/CD20/CD56), CD141, HLA-DR, CD123, CD11b, CD1c, CD11c, CD33, CD34 and CD45. Plasmacytoid (pDC), CD1c<sup>pos</sup> and CD141<sup>pos</sup> myeloid dendritic cells (mDC) were gated as depicted.

(B) Definition of monocyte subsets. Peripheral blood from healthy donors or septic patients was stained for HLA-DR, CD115, CD14, CD16, CD3, CD335 and CD45. After exclusion of CD14<sup>neg</sup>HLA-DR<sup>neg</sup> granulocytes (E1) and CD3<sup>pos</sup>/CD335<sup>pos</sup> lymphocytes and NK cells, the three main monocyte subsets were gated as depicted. For the gating of CD14<sup>pos</sup>HLA-DR<sup>low/neg</sup>/monocytic myeloid derived suppressor cells (M-MDSCs), HLA-DR threshold was defined in a cohort of healthy donors.

(C) Definition of low-density granulocytes (LDGs)/granulocytic (G)-MDSCs. Freshly isolated PBMCs were stained for CD14, HLA-DR, CD3, CD16, CD15 and CD45. CD3<sup>pos</sup> T cells were colored in blue. CD14<sup>pos</sup> monocytes were colored in orange. Finally, CD14<sup>neg</sup>CD15<sup>pos</sup> LDGs/G-MDSCs were colored in green.

(D) Definition of granulocyte subsets. After Ficoll density centrifugation, the PBMC fraction including LDGs and the pellet including high-density granulocytes (HDGs) were stained for CD66b, CD35, CD11b, CD63, CD16, CD15 and CD45. After exclusion of monocytes and eosinophils, CD15<sup>pos</sup> granulocytes were divided into CD11b<sup>neg</sup>CD16<sup>neg</sup> promyelocytes (PM), CD11b<sup>pos</sup>CD16<sup>neg</sup> myelocytes (M), CD11b<sup>pos</sup>CD16<sup>low</sup> metamyelocytes (MM) and CD11b<sup>pos</sup>CD16<sup>pos</sup> mature polymorphonuclear cells (PMN) (E2).

The gating strategies are shown for representative samples.

### **Figure E2. Hierarchical clustering of MDSC-related genes among septic patients**

Hierarchical clustering of 44 immune-related genes, in severe sepsis and septic shock patients. The level of expression of each gene was determined on whole blood RNA by qRT-PCR (TLDA) in 15 patients with septic shock and 14 patients with severe sepsis, and analyzed by unsupervised hierarchical clustering with Spearman's rank distance and average linkage. Color intensity is related to the expression fold change; red = increased expression, green = decreased expression, black = no significant variation.

### **Figure E3. Monocyte HLA-DR expression**

(A) HLA-DR expression on CD14<sup>pos</sup> monocytes. Mean fluorescence intensities obtained with anti-HLA-DR antibody (dark) vs. isotypic control (white) after gating on peripheral CD14<sup>pos</sup> monocytes. Histograms showing representative healthy donor (HD) and septic patient (Sepsis).

(B) HLA-DR expressed as the ratio of mean fluorescence intensity (rMFI) obtained with anti-HLA-DR antibodies vs. isotypic control after gating on the three monocytic subsets in 21 healthy donors (HD) (white boxes) and 28 septic patients (grey boxes).

(C) Proportion of low density granulocytes (LDGs) among PBMCs over 14 days in 10 septic patients. Points = median, bars = interquartile range. Dashed line represents the median of healthy donor values.

(D) Peripheral CD14<sup>pos</sup>HLA-DR<sup>low/neg</sup> cells count and proportion of CD15<sup>pos</sup> LDGs among PBMCs according to Gram stain. Box = interquartile range and median, whiskers = range, points = outlying values.

Comparisons between groups were performed using Mann-Whitney *U* test. \**p*<.05, \*\*\* *p*<.001.

### **Figure E4. Dendritic cells and lymphocyte subpopulations in septic patients**

(A) Comparison of circulating dendritic cells subsets between septic patient (n=33) and healthy donors (HD, n=26), as determined by flow cytometry.

(B) Plasma levels of IL10 and IL12 were determined using a multiplex Luminex assay in 10 healthy donors (HD) and 23 septic patients.

(C) Lymphocyte subset counts were determined on a white blood cells differential by flow cytometry in 88 septic patients and 44 healthy donors (HD).

Box = interquartile range and median, whiskers = range, points = outlying values; comparisons between groups were performed using Mann-Whitney *U* test. \*\* *p*<0.01, \*\*\*\* *p*<0.0001. Ly, lymphocytes; mDC, myeloid dendritic cells; pDC, plasmacytoid dendritic cells.

### **Figure E5. CD14<sup>pos</sup> monocytes and CD15<sup>pos</sup> low-density granulocytes suppress *in vitro* T cell proliferation in septic patients.**

Fresh PBMC obtained from septic patients were magnetically depleted of CD14<sup>pos</sup> cells (PBMC-CD14<sup>pos</sup> cells), of CD15<sup>pos</sup> low-density granulocytes (PBMC-CD15<sup>pos</sup> cells), or not depleted (PBMC), and stimulated with anti-CD3/anti-CD28 antibodies after CFSE labeling.

CD4<sup>pos</sup> and CD8<sup>pos</sup> T-cell proliferation was determined at day 4 by flow cytometry. Representative histograms of 8 independent experiments are shown.

***Figure E6. Flow cytometric characterization of low-density granulocytes.***

(A) Expression of myeloid markers by LDGs. The level of expression of myeloid markers on LDGs (dark histograms) or negatively stained cells (white histograms) was determined by flow cytometry.

(B) Low-density granulocytes (LDGs) have decreased side and forward scatters (SSC and FSC) compared to high-density granulocytes (HDGs). SSC/FSC plots showing structure and size of LDGs compared to HDGs in a representative septic patient (left). HDGs and LDGs were gated on the basis of their CD15 expression within density-segregated interface and pellet cells, respectively. FSC and SSC histograms comparing LDGs (red lines) and HDGs (blue lines) in a representative septic patient (right) are shown.

## SUPPLEMENTAL REFERENCES

- E1. Abeles RD, McPhail MJ, Sowter D, Antoniadou CG, Vergis N, Vijay GKM, Xystrakis E, Khamri W, Shawcross DL, Ma Y, Wendon JA, Vergani D. CD14, CD16 and HLA-DR reliably identifies human monocytes and their subsets in the context of pathologically reduced HLA-DR expression by CD14hi/CD16neg monocytes: Expansion of CD14hi/CD16pos and contraction of CD14lo/CD16pos monocytes in acute liver fail. *Cytometry* 2012;81A:823–834.
- E2. van Lochem EG, van der Velden VHJ, Wind HK, Marvelde te JG, Westerdal NAC, van Dongen JJM. Immunophenotypic differentiation patterns of normal hematopoiesis in human bone marrow: Reference patterns for age-related changes and disease-induced shifts. *Cytometry* 2004;60B:1–13.

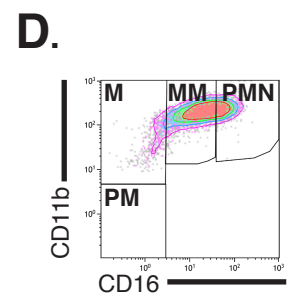
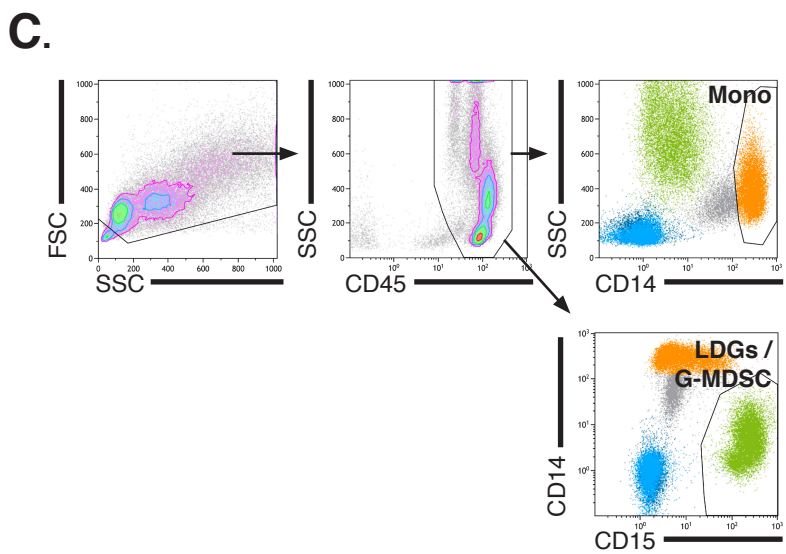
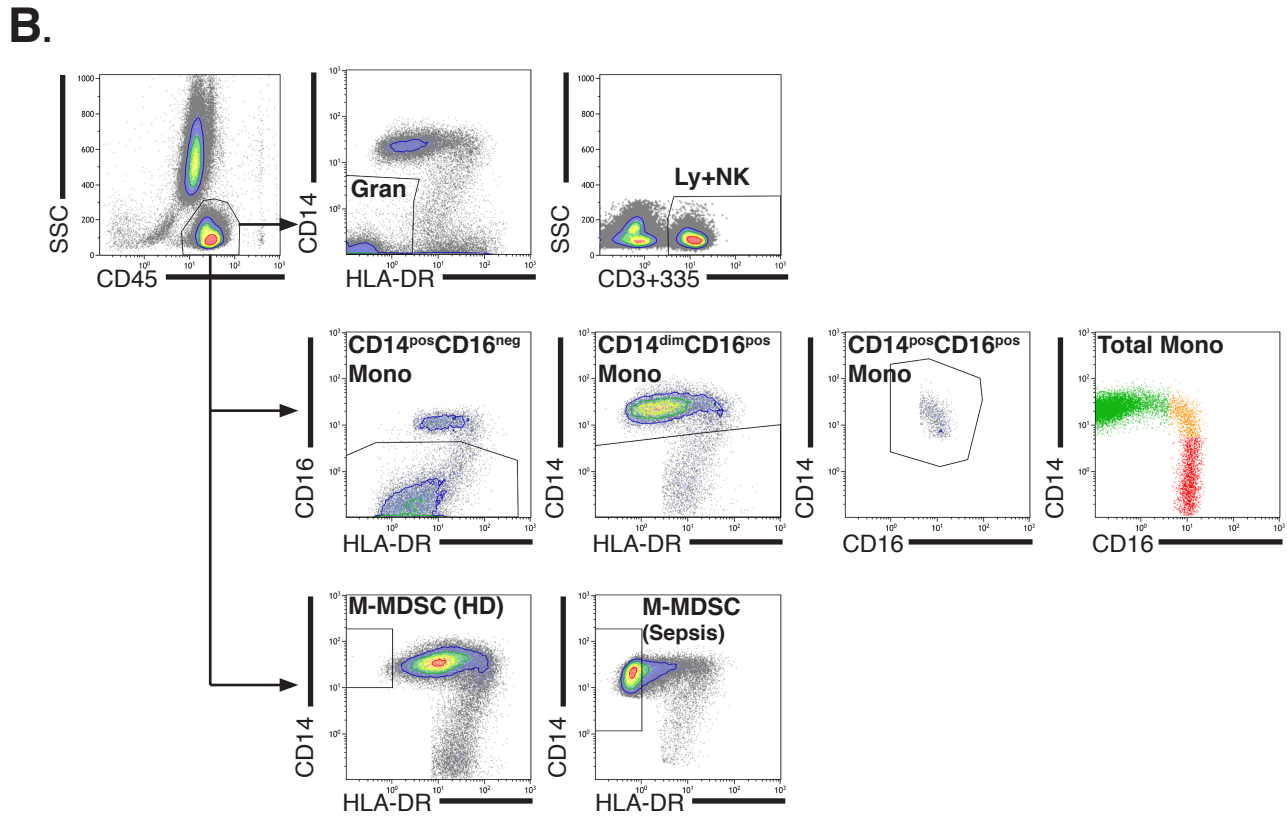
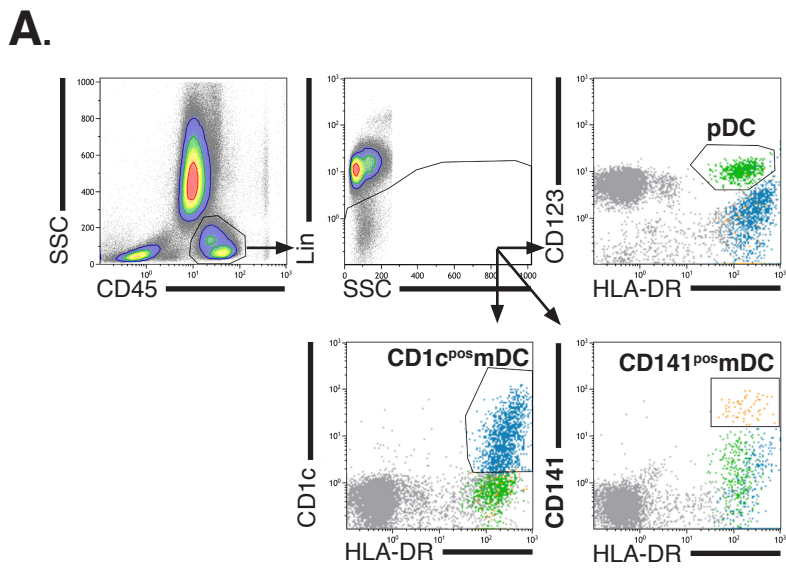


**Figure E1**

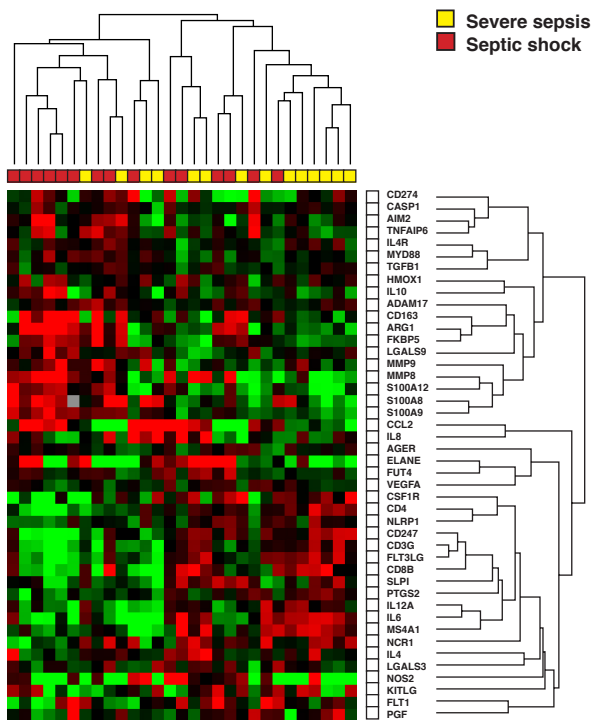
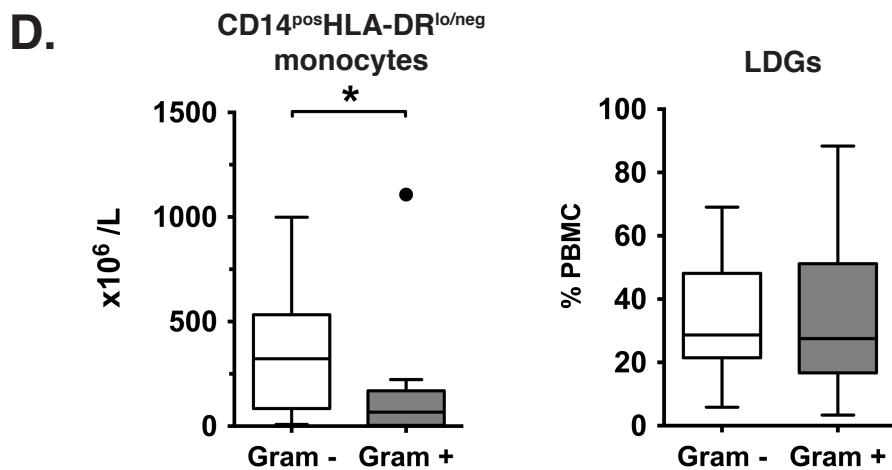
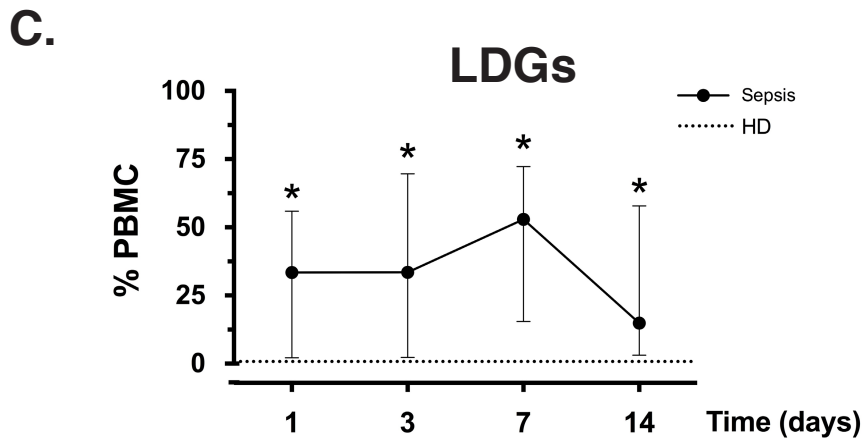
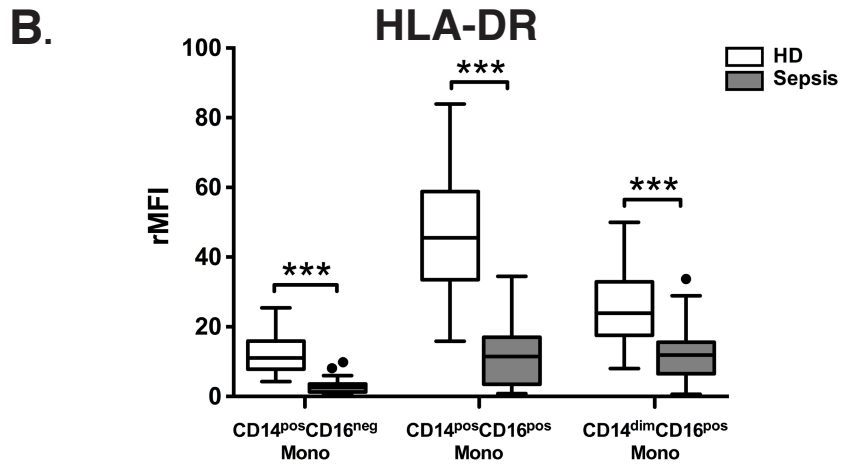
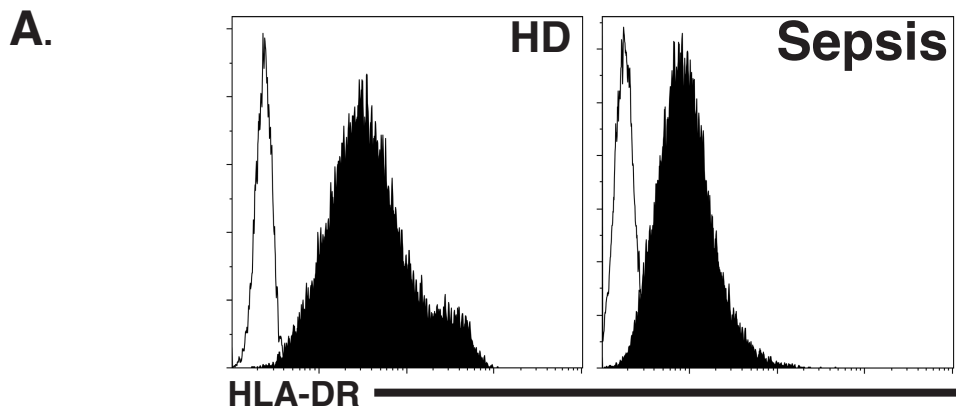
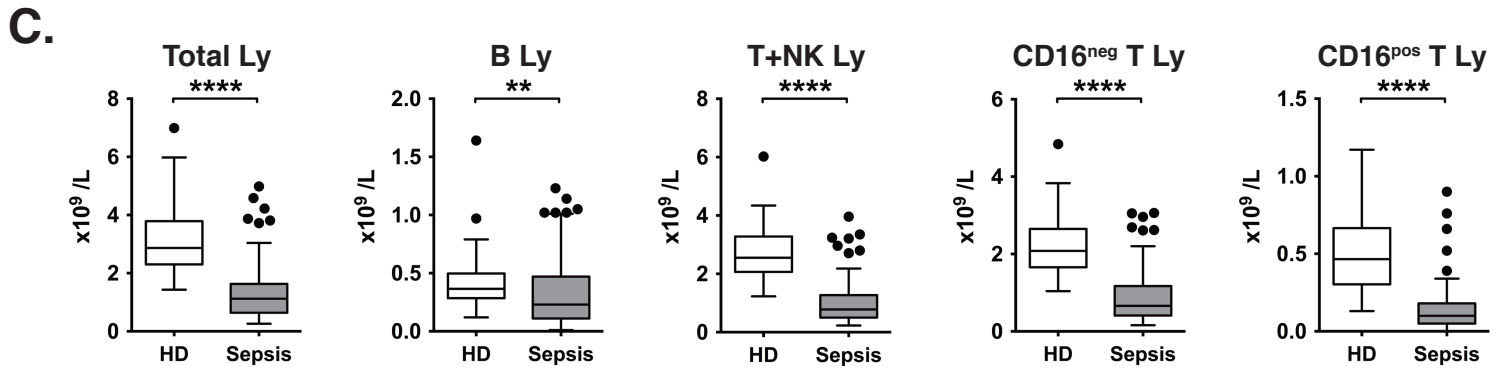
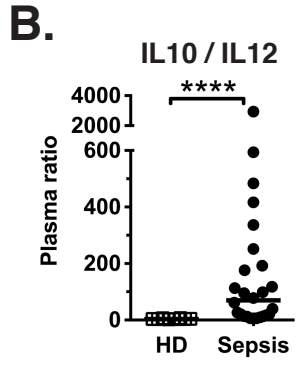
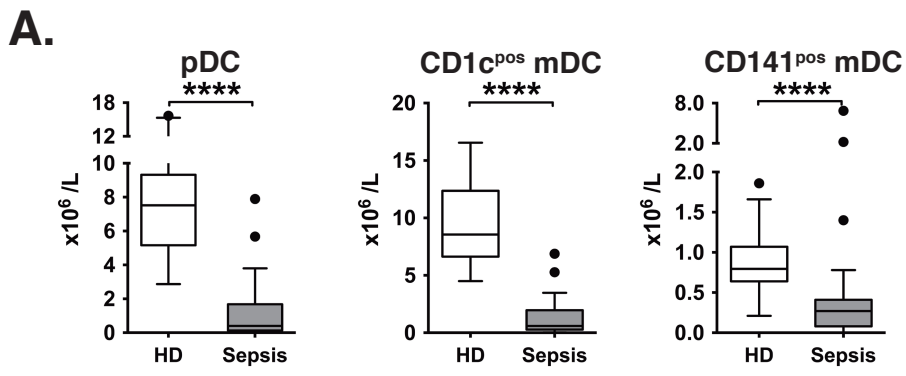


Figure E2



**Figure E3**

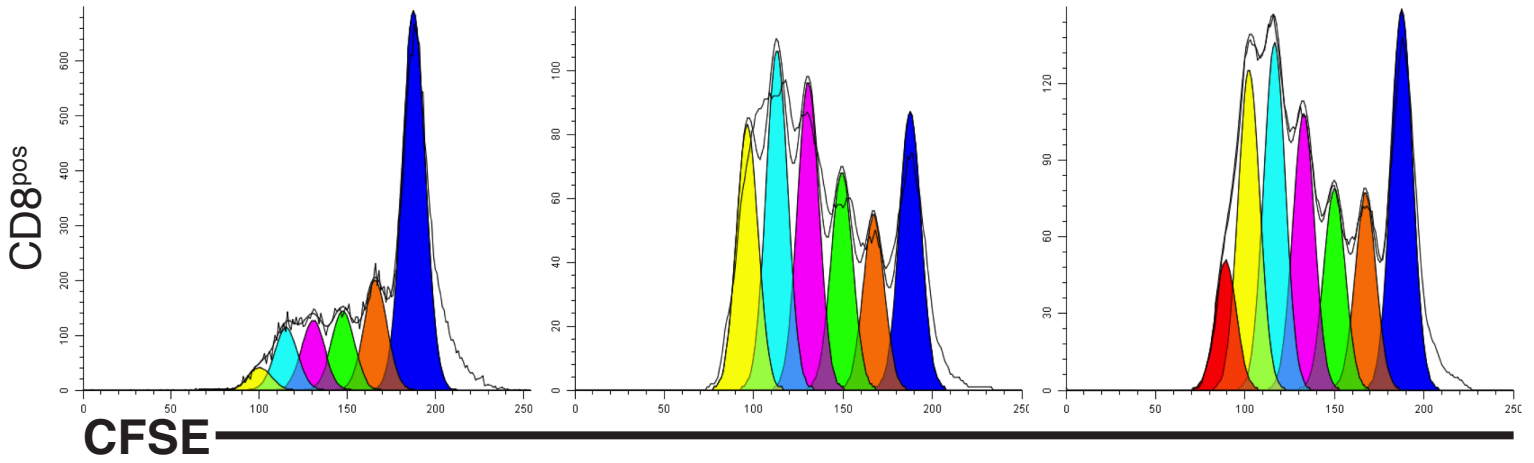
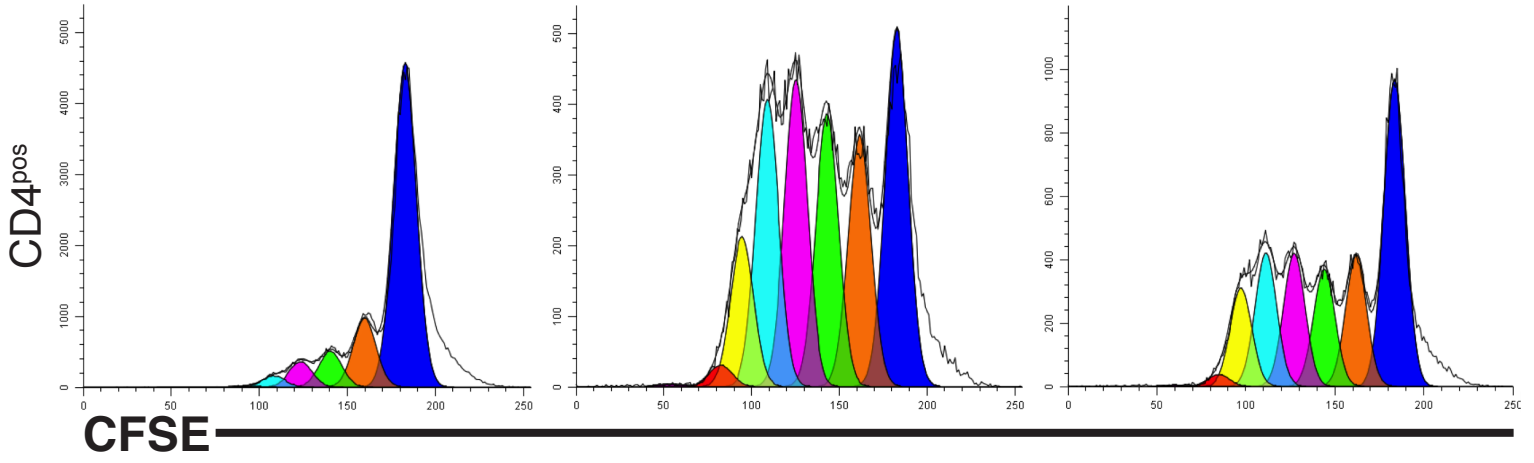


**Figure E4**

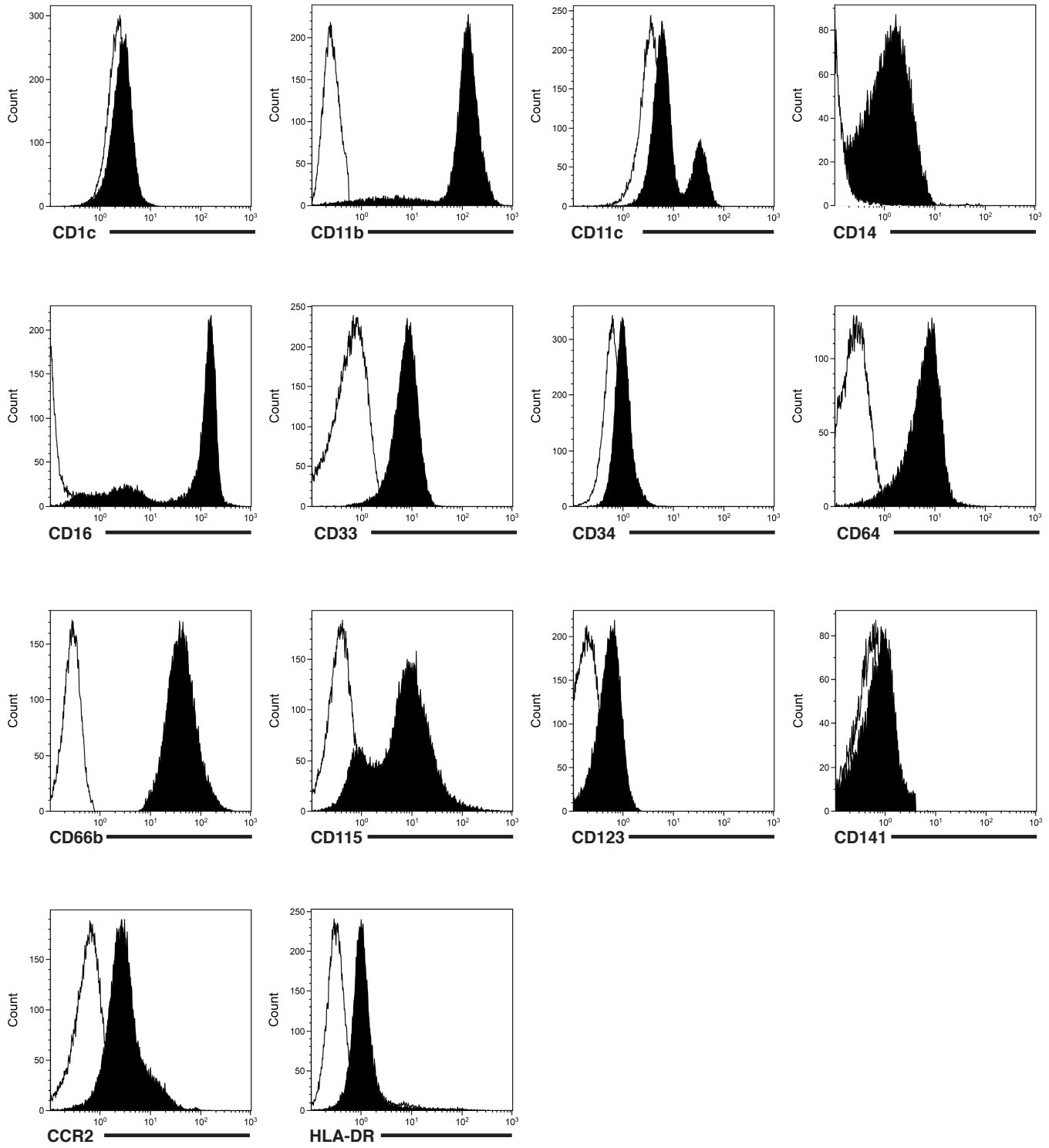
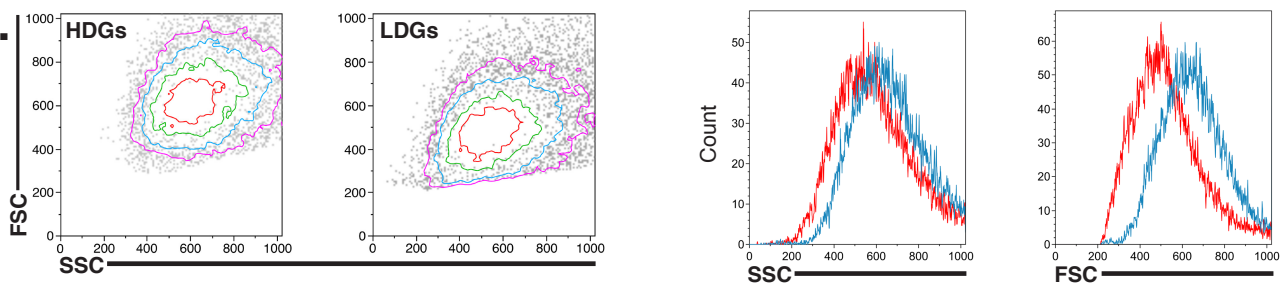
**PBMC**

**PBMC-CD14<sup>pos</sup> cells**

**PBMC-CD15<sup>pos</sup> cells**



**Figure E5**

**A.****B.****Figure E6**